Available online at www.jourcc.com

Journal homepage: www.JOURCC.com

Journal of Composites and Compounds

Carbon-based materials and their composites as Li-ion battery anodes: A review

Belma Fakić [a], Aniket Kumar [b], Mohammad Alipour [c], Aqeel Abbas [d], Elahe Ahmadi [e], Nastaran Nikzad [f], Parisa Shafiee [g]*

[a] *Metallographic laboratory, Institute "Kemal Kapetanović" in Zenica, University of Zenica, B and H*
[b] *School of Engineering & Technology, Shobhit University, Meerut, India*
[c] *Department of Chemistry, Angstrom Uppsala University, Uppsala, Sweden*
[d] *Department of Materials science and Engineering National Taiwan University, Taiwan, China*
[e] *Department of Materials Engineering, Tarbiat Modares University, Tehran, Iran*
[f] *Department of chemistry, Sharif University of Technology, Tehran, Iran*
[g] *School of Chemical, Petroleum and Gas Engineering, Iran University of Science and Technology, Tehran, Iran*

ABSTRACT

Providing powerful, sustainable, and green energy sources is one of the most difficult challenges for maintaining a cleaner environment today. Rechargeable lithium-ion batteries (LIBs), as effective energy storage devices, have gained lots of attention because of their relatively low self-discharge rate, high energy density, and rapid response. Since the efficiency of LIBs is significantly dependent on electrode materials, special consideration has been given to the design of different electrodes. Carbon-based materials are considered as promising LIB anode materials because of their unique structural, electrical, and mechanical properties. Nonetheless, more research is still needed to identify most optimal carbonaceous materials for improving the electrochemical, thermal, and mechanical properties of anodes. In this regard, transition metals and silicon (Si), as high-capacity materials, can be combined with carbon to create high-potential LIBs. This paper reviews various carbonaceous materials and their composites used as LIB anodes. Finally, present challenges and future outlook on these anodes are presented.

Peer review under responsibility of JCC Research Group

ARTICLE INFORMATION

Article history:
Received 25 March 2022
Received in revised form 29 May 2022
Accepted 13 June 2022

Keywords:
Carbon materials
Composites
Lithium-ion batteries
Anodes
Cathodes

Table of contents

* *Corresponding author: Elahe Ahmadi; E-mail: elaheahmadi71@gmail.com*
https://doi.org/10.52547/jcc.4.2.7

1. Introduction

Energy consumption is constantly increasing as a result of economic and population growth, as well as the development of agriculture and industry. [1]. The economic development of a country is directly reflected by the relentless increment in energy consumption in various sectors. The main challenges to energy sustainability are the finite nature of nonrenewable energy sources and the need to limit carbon dioxide emissions. Hence, eco-friendly alternative energy sources such as hydropower, wind energy, solar cells, etc. have been broadly examined. Nonetheless, because of the unpredictable nature of such electricity generation sources, a proper technology for effective energy storage and distribution is needed [2-4]. Among different energy storage systems, rechargeable (secondary) batteries, which store electrical energy in a form of chemical energy, are regarded as one of the most effective and practical methods for the electric power management as well as the integration of renewable energy generation with grid applications [5, 6]. LIBs are the most commonly used ones. They present higher operating voltages, no memory effect, lower maintenance requirements, higher energy density, long cyclic life, and limited self-discharging relative to other rechargeable batteries, including nickel-metal hydride and nickel-cadmium batteries [7-9].

Graphite is the current commercial anode used in LIBs. However, it cannot fulfill the great demand for high power/energy density and improved cyclic performance required for a variety of applications, including electric devices, transportation, and stationary energy storage systems. They have a relatively low theoretical capacity (372 mAh/g) and serious safety issues because of the lithium plating and subsequent Li-dendrites formation on the graphite surface [10, 11]. Hence, considerable efforts have been invested in developing a new generation of anodes with proper charging-discharging potential, high capacities, low manufacturing costs, and better safety [12-15].

Carbon-based materials including graphene, carbon nanofibers (CNFs), carbon nanotubes (CNTs), and their composites have been extensively investigated as LIB anode materials. Relative to conventional electrodes, such as activated carbons (ACs) or graphite, these kinds of carbonaceous materials differ in morphology, dimensionality, and also in chemical bonding distribution, allowing mixtures of local electronic structures between sp^3 and sp^2. Hence, they exhibit different carrier-transport properties from classic carbonaceous materials, in reactants' contact time. These novel materials with short ion diffusion length and high available surface area offer a new perspective for high power/energy density devices [16]. Several reviews have been published on the advancement of LIB anodes from different perspectives [10, 17-19]. Nonetheless, various carbonaceous anode materials and their composites have not been comprehensively explored. The current review gives an overview of the development in technologies for Li-ion storage concerning the usage of carbon-based materials and their composites. This paper is organized as follows: a brief discussion on the LIB cell, LIB anode materials, and the introduction of carbonaceous anodes and their composites.

2. Li-Ion Cell Components

Li-ion system generally comprises three parts: conducting electrolyte, cathode, and anode (Fig. 1). Anode is commercially made up of graphitic carbon, acting as a negative terminal, and cathode is typically composed of a lithium metal oxide, being the positive terminal of the cell. Li-intercalation compounds are the form of energy storage in the electrodes. Dissolved lithium salt (Lithium bis-oxalate borate (LiBOB) or Lithium hexafluorophosphate ($LiPF_6$)) in an organic solvent (dimethyl carbonate or ethylene carbonate) is commonly employed as a conducting electrolyte. In an ideal LIB, the number of transferred Li-ions in the electrolyte should be united. The cathode and anode react according to the following half-reactions (in mole units), respectively:

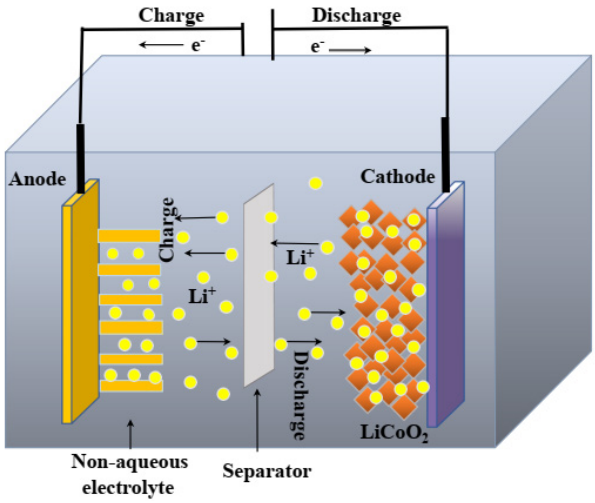

Fig. 1. Schematic of Li-ion cell.

$$LiMO_2 \leftrightarrow xLi^+ + Li_{1-x}MO_2 + xe^- \quad (1)$$

$$6C + xLi^+ + xe^- \leftrightarrow Li_xC_6 \quad (2)$$

where, M denotes the metal used to form lithium metal oxide, and x represents the coefficient (typically 1) for a complete reaction.

Upon charging, the half-reactions proceed in the forward direction by the voltage exerted on the electrodes. Metal in $LiMO_2$ is reduced, forming Li-ions and releasing them into the electrolyte. In the following, the ion diffusion via the electrolyte and their insertion into the graphite anode occur. Besides, to maintain the charge neutrality, free electrons are also generated, subsequently conducting through a wire connected to electrodes. This provides the necessary electrons needed to insert Li-ions into the anode. Upon discharging, the reaction occurs reversely and the electrons pass from the anode to the cathode via the external load derived from the potential difference between the electrodes. This leads to originate a positive current from the cathode, acting as a positive terminal of the cell [20-22]..

3. An Overview of LIB anode materials

An ideal LIB anode need to meet the requirements of high reversible volumetric and gravimetric capacities, low potential against cathode materials, long cycle life, high-rate capability, environmental compatibility, excellent abuse tolerance, and low cost. [22]. At the early development of LIBs, the most widely used anode was graphite. However, as mentioned above, several intrinsic drawbacks have limited their applications. Hence, further advancements in LIB anode materials are required to develop portable high energy-consuming devices [17].

Among all potential anodes for LIBs, Si is considered the promising alternative to graphite because of: (1) an appropriate discharge voltage (~ 0.2-0.3V vs. Li/Li+) which is able to adequately pair up with commercial $LiFePO_4$, $LiCoO_2$, etc. cathode materials and avoid adverse Li-plating process; (2) high theoretical specific capacity (4200 mAh/g for $Li_{4.4}Si$); and (3) being eco-friendly, inexpensive and naturally abundant [11, 23-25]. However, during the Si lithiation/delithiation process,

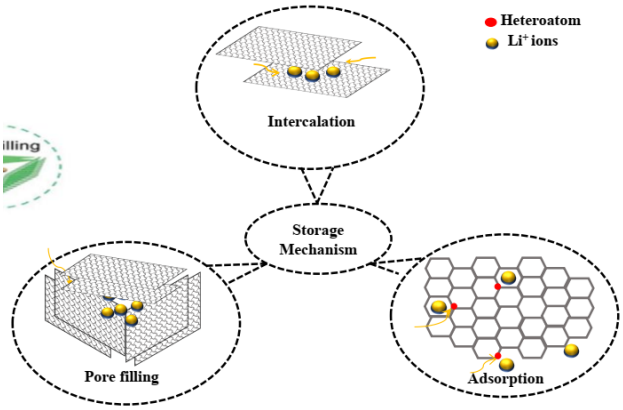

Fig. 2. Schematic of storage mechanisms of Li-ions in HCs.

huge stress is generated by excessive volume expansion (~360% for Li4.4Si). This causes a series of intense destructive outcomes, which include the disconnection between the current collector and electrode via the interfacial stress, deterioration of electrode structure integrity resulting from the gradual increase of pulverization during repeated charge-discharge processes, and continuous Li-ion consumption during constant solid electrolyte interface (SEI) layer formation–breaking–reformation process [25-32]. In this regard, capacity fading and electrode collapse are accelerated in a synergistic way by all these processes. In addition, the weak intrinsic electron conductivity and volume expansion problem of Si contribute to the sluggard electrochemical kinetics [33].

The other promising candidate to substitute graphite is the conversion electrode materials owning to their high specific capacity [34]. These groups mainly refer to the transition metal oxides (TMO), and also include the metal nitrides and sulfides. Nonetheless, same as alloy anodes (Si), these anodes have the problems of volume and morphology changes at the whole electrode level, unstable SEI layer, and pulverization of materials at the individual particle level. The great voltage hysteresis (~1V) of conversion anodes between charge-discharge is another challenge, which should be addressed [22]. Despite the significant progress that has been made in designing novel anode materials for LIBs, carbon-based materials still remain very favorable anodes because of their good features, which are investigated in the next sections.

4. Carbon-based materials

Carbon or its compounds are a significant aspect of nature [35]. Different carbon-based materials have been theoretically and experimentally studied for conversion and energy storage devices like supercapacitors [36-39], LIBs [40-42], and fuel cells [43-46] to improve their lifetime, cyclic efficiency, power, and energy densities, and specific capacity. They were also used as the electrocatalyst [47], and biosorbent [48].

A special combination of chemical and physical properties including low cost, ease of accessibility, thermal, chemical, and electrochemical stability, and good lithiation-delithiation reversibility is the underlying reason for the usage of these materials to enhance the storage device electrodes' performance. Currently, research activities are strongly concentrated in graphene, CNTs, porous carbon, and CNFs as the most promising carbonous anodes. The reduced size and special shape of these structures offer unique features that significantly enhance the capacity of energy storage [8, 49-51].

4.1. Hard carbon (HC)

HC has been well-proven to be electrochemically active and provide desirable performance in alkali metal-ion batteries [52, 53]. The specific capacity of up to ≈1000 mAh/g can be obtained by HC in LIBs (approximately three times greater than that of graphite anodes), which is appropriate for LIBs with high energy density [54]. Further, a low-voltage plateau of HC anode with a significant amount of capacity make it able to deliver high power density in LIBs [55]. In general, the voltage profile is mainly divided into two regions including a sloped region with the capacity of 150–250 mAh/g in the 1.0–0.1V voltage range and a plateau region with the capacity of 100–400 mAh/g [56]. Furthermore, because of the three-dimensional (3D) pathways for ion transfers in the structure, HC offers better rate performances than graphite [55]. A high potential for low production costs is another attractive feature of HC. In fact, it can be produced by a wide variety of precursors such as commercially available polymers, worn-out tires, recycled electronic circuit boards, and renewable biomass materials. Direct precursor pyrolysis for HC synthesis is a relatively easy and scalable process [57-59]. Hence, due to their low expansion rate and working potential of the electrode, improved cycling stability, high capacity, and outstanding capacity retention, HC is becoming preferred anode for next-generation LIBs in high power applications.

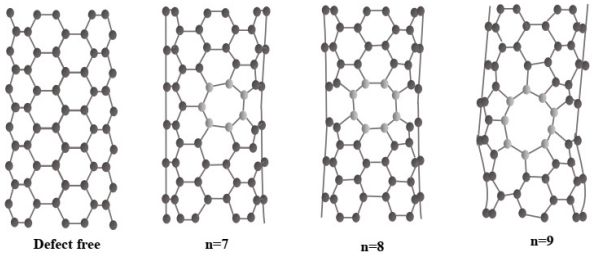

Fig. 3. Schematic of defects types in CNTs.

HC, known as non-graphitizable carbon materials, has a random alignment of graphene sheets and is unable to reshape into graphite even at temperatures above 3000°C. The formation of covalent C-O-C or cross-linking bonds in precursors can be responsible for its non-graphitizability. During pyrolysis, rigid cross-linking structures, oxygen-containing functional groups, defects, and micropores are formed. These significantly eliminate the growth of graphite sheets [60-62]. The most accepted structural model for HC is falling cards presented by Dahn et al. [63]. This model offers the presence of amorphous regions with nanopores and defects, and small graphene sheets with a limited lateral dimension of 40Å, which are ordered in short range. The paralleled layers of graphitic domains have been shown to be turbostratic, bent, or curved than flat. The spacing of (002) interlayer of graphitic layers in HC is 3.6–4.0 Å, which is larger than that of graphite (3.35Å). It can be expanded by introducing heteroatoms or controlling the synthetic conditions [60].

The complicated and important constituents of HC are nanopores which are either closed or open in the HC matrix. Large specific surface area is resulted from the open pores, leading to weak initial Coulombic efficiency (ICE) because of the excessive formation of SEI [64]. Though closed pores are preferred because of providing active sites for alkali metal-ions accommodation, the SEI layer formation is also reported in the closed pores of HC by in situ small-angle neutron scattering [65]. Because determining the size and number of closed pores is challenging, it is difficult to relate the performance of HC to the pore structures. The HC structures also contain defective sites, edges, and vacancies. Though the majority of carbon atoms are present in the six-membered ring systems, some heptagonal or pentagonal defective sites also exist [66]. The defect content is also diverse, depending on the precursor properties. Relative to the HC derived from high-molecular-weight precursors, more defects can be attained by those derived from medium molecular weight precursors with medium molecular weight [67]. Cao et al. [68]

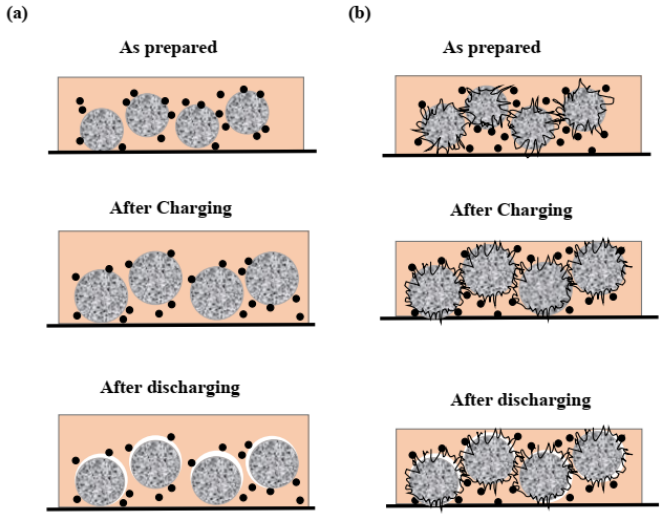

Fig. 4. Schematic of failure modes in (a) Si, and (b) Si-CNTs electrodes.

showed that the crystalline size of HC also affects the content of defects, presenting more defects with smaller crystalline size. Heteroatoms including K, O, N, P, B, S, and F have been frequently reported as the defective sites in the structures of HC [69-73]. These special structural features make the Li-ion transport length shorten and offer many active sites for charge transfer reactions.

Based on the Li-ions storage mechanisms, they are classified into the following three categories, including (1) Li-ions absorption at the defect sites, (2) Li-ion intercalation into the graphitic layers, and (3) Li-ions uptake in the nanopores (Fig. 2) [64].

Early research suggested that the Li intercalation into the graphitic domains derives from the sloping region in the discharge-charge curves. Stevens [74] and Dahn [75] investigated HC structural evolutions during the insertion of Li. The Li-ions intercalation into the graphitic domains at the sloping region is proposed by in situ X-ray diffraction analysis with a reduction in the (002) peaks intensity. At the low potential plateau, an increase in electron density is demonstrated by in situ small-angle X-ray scattering. This can be derived from the nanopores filling. The suggested intercalation-pore filling mechanism is supported by these results. In this mechanism, the plateau and sloping regions are ascribed to the Li nanopores filling and Li-ions intercalation into the pseudo-graphitic sheets, respectively. In recent studies, more evidence that assigns the sloping region of HC to the Li-ions adsorption at the edge or defect sites and the plateau region to the Li intercalation into the pseudo-graphitic layers are revealed [54, 62]. The adsorption-intercalation mechanism for Li-ion storage is supported by a recent in situ Raman analysis [54].

However, HC has two major limitations, including low tap density and low ICE. Several strategies have been employed to overcome these drawbacks such as using a thin layer of soft carbon or metal coating or through fluorination, and surface oxidation [76, 77]. In particular, better LIB performance resulted from a soft carbon thin layer by improving both the capacity and the Coulombic efficiency [76]. In addition, both the cycling life and the Li-ion storage capacity of HC still require to be improved. In this regard, to enhance the capacity, HCs with porous structures were synthesized [78]. Li et al. [79] used potato starch to synthesize the micron-sized HC which showed well rate capability and cycling life with about 530 mAh/g reversible capacity. Similarly, Yang et al. [80] employed pyrolyzed sucrose to prepare nanoporous HCs and evaluated their electrochemical performances. A good cycling life and rate capability along with a considerable capacity close to 500 mAh/g were presented by these nanoporous materials. The high-rate capability was ascribed to the fast Li diffusion (4.11×10-5 cm^2/s) for the hierarchical nano-porous structure of HC.

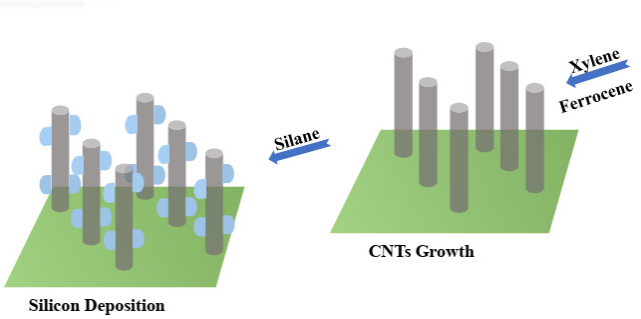

Fig. 5. Schematic of nanostructured Si/CNT synthesis.

4.2. CNTs

Owing to their high tensile strength of up to 60 GPa, high conductivity (106 S/m and >105 S/m at 300 K for single-walled (SWCNTs) and multi-walled CNTs (MWCNTs), respectively), high rigidity (Young's modulus on the order of 1 TPa), specific structure (rolled Graphene sheets piled in the cylindrical/tubular structure) [21, 81, 82], CNTs have been considered as the potential LIB anode materials [21].

The Li-ions storage mechanisms in CNTs have been widely studied [16]. In the first-principles studies, the nature of Li intercalation in the CNT ropes was investigated. The obtained results revealed a charge transfer between carbon and Li, as well as, a slight CNT structure deformation because of the intercalation. Li intercalation was discovered to be possible in both the interstitial and interior spaces of the nanotubes [83]. Ab initio studies on Li intercalation through the cap region or sidewall of CNTs indicated that the energy barrier of Li insertion is dependent on the carbon ring size. The outside the tube and inside the tube near the wall were preferred positions for Li insertion [84].

Intercalation capacity in CNTs is no longer restricted to LiC_6 and is closely related to the nanotube morphology [85, 86]. It is mainly affected by the naturally-occurred or artificially-induced defects [86, 87]. The researchers have quantified the defects caused by carbon atoms removal from the ordered hexagon rings, which create a hole in the side walls. The hole is found to be broadened by simultaneously removing more carbon atoms. Li can simply diffuse inside the nanotubes with three removed carbons (n=9), while it scarcely diffuses to the interior of defect-free nanotubes (n=6) and nanotubes with one (n=7) and two (n=8) removed carbon atoms (Fig. 3). The diffused Li-ions freely move through the interior of the CNTs and can accumulate [88-90].

CNTs can be treated with acids like nitric acid to introduce defects. In addition to the common intercalation between the graphene layers, chemical etching introduces additional electrochemical active sites including microcavities, edges of graphitic layers, disordered graphitic structures, and defects, enhancing the Li storage capacity of MWCNTs. In this regard, a significant increase in the first discharge capacity of MWCNTs from 312 mAh/g to 2087 mAh/g was reported through the chemical etching [30]. Defects in CNTs can also be introduced by ball milling. In general, ball-milling has been considered a useful approach for improving the electrochemical properties of CNTs. Eom et al. [91] investigated the impact of high-energy ball-milling on the properties of Li intercalation of MWCNTs synthesized by the Chemical vapor deposition (CVD). An increase in the ball-milling time was accompanied by increasing the reversible capacity and decreasing the irreversible capacity from 351 and 1012 mAh/g for purified MWCNTs to 641 and 518 mAh/g for ball-milled ones, respectively. This irreversible capacity reduction led to the Coulombic efficiency increment. Furthermore, the stability of ball-milled MWCNTs were more than the purified ones. The fractured graphene layers' edges and the surface functional groups chemically linked to these edges were thought to be responsible for increasing the reversible capacity of ball-milled MWCNTs [91]. Gao et al.

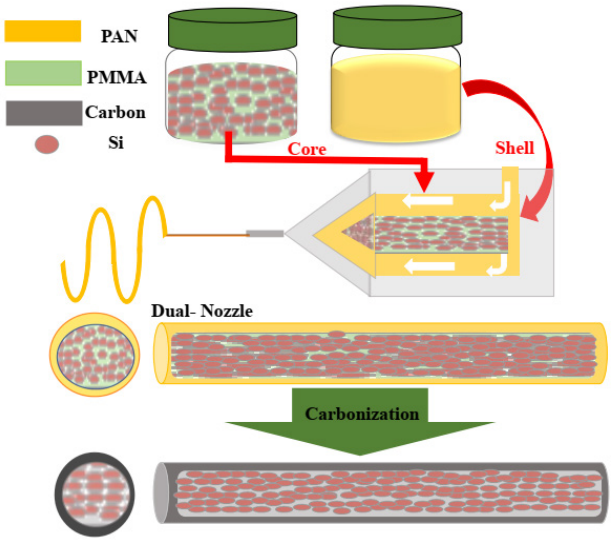

Fig. 6. Schematic of Si nanoparticles/CNFs fibers fabrication via a dual nozzle electrospinning equipment.

[92] compared the properties of electrochemical intercalation of as-prepared, filtered, and ball-milled SWCNTs, showing reversible capacities of 450 mAh/g ($Li_{1.2}C_6$), 600 mAh/g ($Li_{1.6}C_6$), and 1000 mAh/g ($Li_{2.7}C_6$), respectively.

Ends of open-ended CNTs are the other pathways for Li entrance. For instance, the capacity difference between opened and unopened CNTs was determined to be almost 120 mAh/g [93]. However, to be effective in this approach, tailoring the CNTs to shorter tubes is needed. This allows ions to enter and exit freely [94]. Shimoda et al. [86] reported an increase in the reversible capacity from LiC_6 for closed-ended tubes to LiC_3 after etching because of the shortening and introducing defects into the CNTs. The length of the CNTs can be also reduced via ball milling. Yang et al. [95] compared the electrochemical properties of two kinds of CNTs -long (LCNTs) and short (SCNTs). SCNTs revealed a capacity of 266 mAh/g, which was approximately two times higher than that of LCNTs. Because of the surface resistance of nanotubes and the surface functional groups in the CNTs, LCNTs showed larger voltage hysteresis. In addition, according to AC impedance results, relative to SCNTs (3–4 Ω), LCNTs had a higher charge transfer resistance (31.2– 61.2 Ω). In general, short CNTs have two advantages over longer nanotubes including presenting more edges per unit length and fascinating the entry and exit of Li ions to and from the nanotube's interior. These provide easier Li-ion intercalation/deintercalation into/from the graphitic layers.

Many attempts have been made to substitute graphite in LIBs with pure CNTs. Nonetheless, a slight improvement in the graphite capacity is provided by raw CNTs. Besides, CNTs face problems such as difficulty in consistently controlling their morphology and structure during synthesis, and high irreversible capacity. As a result, employing the pure CNTs as the substitution for graphitic anodes is currently difficult to justify [21].

4.3. Graphene

Graphene is composed of a single layer of sp^2 hybridized carbon atoms with nanometer thickness arranged in a two-dimensional honeycomb lattice. Since its discovery in 1987, graphene has gained a lot of interest due to its unique features and adaptability in different fields, including physical, chemical, engineering, and biological sciences [96-101]. High mechanical strength, good conductivity, high surface area, and high carrier mobility of graphene have made it a promising LIB anode material [16, 102]. However, theoretical investigations on the graphene's lithium storage are quite contentious. Although, the amount of Li absorbed on the single-layer graphene is lower over the graphite [103], as a set of graphene sheets are held together, this amount exceeds the performance of graphite to 780 mAh/g or 1116 mAh/g [104, 105]. These two amounts are related to two different explanations of Li-graphene interaction. In particular, the first one supposes the Li-ions adsorption on the both sides of graphene, whiles the second one supposes the covalent trapping of Li-ions at the benzene ring.

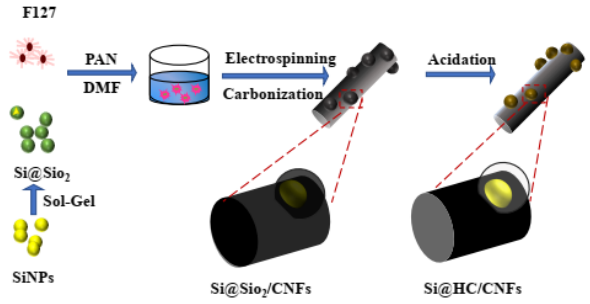

Fig. 7. Schematic of Si@C/CNFs fabrication process.

Interestingly, there are many experimental activities concerning graphene as a LIB anode [36, 106-109]. For instance, Pan et al. [105] synthesized disordered graphene sheets by different means including electron beam irradiation, low-temperature pyrolysis, and hydrazine reduction process. High gravimetric capacity (between 790 mAh/g to 1050 mAh/g) of graphene sheets was reported which was ascribed to the existence of more active sites like edges and other defects for Li storage. In-situ preparation of doped graphene electrodes with hierarchically porous structure possessing long and ultrafast cycling capability for LIBs was reported by Wang et al. [110]. Long cycling capability at 5 A/g current density (about 3000 cycles) and high Li storage were achieved by the usage of these electrodes. These resulted from the synergetic effects of hetero-atom doping, good conductive network, and hierarchically porous structure, facilitating the mass transport and accelerating the electrochemical reactions. Among the graphene materials, promising potential in the capability of Li storage can be obtained by nanoribbons made from MWCNTs. In particular, Fahlman et al. [111] synthesized both oxidized and reduced graphene nanoribbons. The oxidized ones showed a stable capacity of 800 mAh/g and increased Li uptake. Attentively engineered layer spacings between the nanopores, defective sites on the plane of graphene, or reassembled graphene nanosheets, for the diffusion of Li-ions, can be also considered to achieve a good rate capability and high capacity. A capacity in the range of 200-500 mAh/g has been reported for pure graphene sheets reduced by various approaches [112, 113]. To expand the layer spacing in graphene, C60 and CNTs have been introduced and the performance improvement has been achieved in both cases [114]. An increase in anode capacity from 540 mAh/g to 784 mAh/g has been reported by C60 incorporation into the graphene structure [112].

5. Carbon composites

Due to the high demand for electrodes with good rate capability, long cycling life, and high capacity, achieving all of these features with single-phase materials is difficult, even when the dimensions are reduced. As a result, composites have gained much interest as electrode materials for energy storage devices. They can combine the unique features of individual nanostructures with possible synergistic effects [115]. Recently, carbon has been combined with alloy materials like Si, metal sulfides, and metal oxides to form composites.

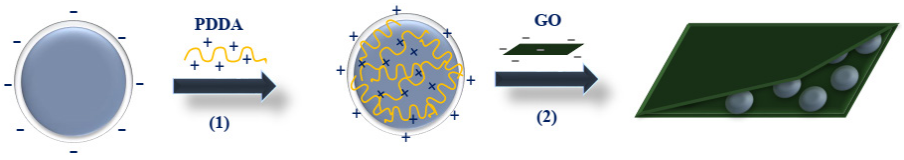

Fig. 8. Schematic of Si/graphene composite fabrication via electrostatic self-assembly approach.

5.1. Si-Carbon composites

5.1.1. Si-CNT/CNF

Currently, CNFs and CNTs are the main nanocomposites with Si [116-119]. In particular, because of several advantages such as impressive thermal and mechanical stabilities, and high electrical conductivity, Si-CNTs composite materials display high potential to use in LIBs [120, 121]. These characteristics are essential for good electrode performance in electrochemical processing.

To prepare Si/CNT composite, the in-situ growth of CNTs via the CVD method has mostly been used [122-124]. In one research, CNTs were directly grown onto the surface of fine Si nanoparticles using the CVD method [125]. Relative to directly mixed Si/CNTs and bare Si electrodes, superior performance was obtained by this electrode. The flexible characteristics and void space of CNTs were thought to accommodate the Si core's volume expansion without severe swelling of the electrode. Fig. 4 shows the principle underlying the improved electrochemical performance by core-shell Si/CNTs composites in comparison with Si powder electrodes consisting of a random blend of carbon black and Si particles. Si particles have tendency to de-bond and separate from the binder after discharging. Hence, for the conventional anode materials, the electrical-conductive networks can simply break during cycling. Superior electrochemical performance can be delivered by the full integration of CNTs with Si particles, forming a core-shell structure. The accommodation of Si (the core of the electrode) volume expansion by the CNT layer minimizes the swelling of the electrode. This results in the maintenance of the electrical-conductive network even with a large volume expansion. The performance of the directly mixed Si/CNT electrode is not equally improved, since CNTs essentially play the same role as the carbon black [10].

Wang and Kumta [126] proposed another interesting concept to prepare Si/CNTs electrode composite. They used a simple two-step CVD technique to vertically align MWCNTs on the quartz slides using ferrocene as the catalyst and xylene as the source of carbon (Fig. 5). Crystalline/ amorphous Si nanoparticles were uniformly deposited onto CNTs with SiH_4 as the source of Si. The homogenous dispersion of Si nanoparticles was facilitated by the space between MWCNTs. This inhibition of agglomeration diminished the strain induced by the Si volume expansion. Besides, the hybrid nanostructure of Si/CNT offered the rapid ion and electron transportation. The hybrid anode presented high Columbic efficiency and high reversible capacity of ~2000 mAh/g over the first charge/discharge cycles. Afterward, a rapid performance loss was revealed in the cycling tests because of the weakening of the Si/CNTs interface, fragmentation of the attached Si nanoparticles, and continuous growth of SEI. As a result, while this hybrid structure avoided the Si particle agglomeration and enabled the ion and electron transportation, it could not address the SEI and pulverization concerns.

To address the weakening of the Si/CNTs interface, Sun et al. [127] functionalized the CNTs using atomic oxygen. This successfully retain the dispersion and regularity by the strong anchoring of Si nanoparticles onto CNTs, which allows uniform layer (~ 15 nm) growth of Si nanoparticles on the functionalized CNTs. An excellent cyclability (capacity retention of 80% after 160 cycles), high areal capacity of 3.86 mAh/cm^2, and high specific capacity of 922 mAh/g were simultaneously attained by the interface-tailored electrodes. These values are among the highest reported. In fact, chemical tailoring of the carbon-Si interface improved the electrical and structural interconnections throughout the whole electrode, resulting in remarkable electrochemical performance.

Despite their excellent performance, the formation of tiny cracks after expansion and contraction is a common stress-related issue in Si core-shell anodes. This can eventually lead to the shell's fracture and separation [128-130]. Introducing a rough Ni layer between Si shell and CNT core can address this issue. Improved adherence and stability, superior charge transport, and better accommodation of stress were obtained by the resulted nanohybrid structure. The electrode presented a capacity over of 2500 mAh/g with a low fading rate of 0.2% per cycle after 110 cycles. Effective charge transfer between Ni and Si was

Table 1.
Li storage performance of Si/carbon composite materials.

Sample	Structure	Preparation Method	Cycling stability	Ref.
nano-Si/carbon	Core–shell	Substrate induced coagulation method	1800 mAh/g over 50 cycles	[163]
Amorphous-Si@SiO_x/carbon	Core–double layer shell	Ball-milling and carbonization	1450 mAh/g at 100 mA/g after 100 cycles	[164]
Fluorine functionalized Si/ carbon	Core–shell	High-temperature pyrolysis method	683 mAh/g at 200 mA/g after 50 cycles	[165]
Si microsphere/carbon	Core–shell	Self-corrosion reaction, annealing, and chemical etching	1027.8 mAh/g at 1 A/g after 500 cycles	[166]
Si/carbon	Core–shell	Esterification, and carbonization	1131 mAh/g at 0.5 A/g over 200 cycles	[167]
Si@graphite/N-doped carbon	Core–shell	Spray-drying process, and two-step heat treatment	611.3 mAh/g at 300 mA/g after 100 cycles	[168]
Si/void/mesoporous carbon	yolk–shell	Stöber sol–gel method, Surfactant-templating sol–gel route, and nano-casting route	1000 mAh/g after 400 cycles	[169]
Si/void/carbon	yolk–shell	Hydrolysis coating, carbonization, and chemical etching processes	617.7 mAh/g after 20 cycles	[170]
Si/void/SiO2/void/carbon	Dual yolk–shell	Stöber method, and chemical etching	956 mAh/g after 430 cycles	[171]
Si/carbon	Porous	Purification, reduction, and pyrolysis	759 mAh/g after 30 cycles	[172]
Si/carbon	Porous	ball milling, spray drying, carbonization and CVD processes,	560 mAh/g after 50 cycles	[173]
Si/carbon	Porous	chemical etching, and calcination method	1287 mAh/g at 100 mA/g after 50 cycles	[174]

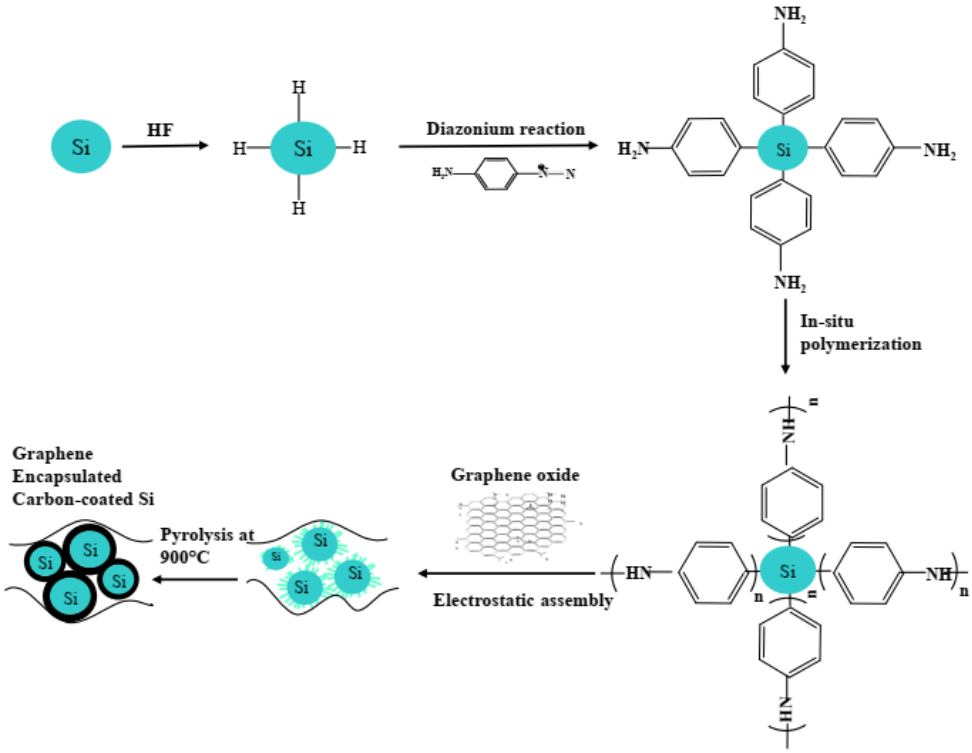

Fig. 9. Schematic of graphene/carbon coated-Si nanoparticles composite fabrication.

thought to be responsible for the improvements [131].

CNFs were firstly made by Thomas Edison via the carbonization of bamboo and cotton. This approach has been developed and employed in both practical settings and scientific studies [132, 133]. The processing conditions and the morphology of the precursor determine the structure of CNFs. They generally show excellent stress resistance, high chemical and thermal stabilities, and good electrical and thermal conductivities which lead to the wide application prospects in hydrogen storage materials, nanoelectronic devices, composite materials, and LIB anode materials [134, 135]. Electrospinning, CVD, or solid-phase synthesis can be used to synthesize CNFs [136-138]. However, CNFs employed for Si-carbon composite anodes are mainly prepared by electrospinning. It is a scalable and low-cost method for the fabrication of Si nanoparticles-CNF composites [139].

Si nanoparticles encapsulation into the CNFs has been considered an effective mean to enhance the Si anode's electrochemical properties. In this regard, Hwang et al. [140] employed the electrospinning method to fabricate Si nanoparticles/CNFs fibers using a dual nozzle (Fig. 6). Into the nozzle's shell channel, Polyacrylonitrile (PAN) dissolved in N, N -dimethylformamide (DMF), and into the nozzle's core channel, poly (methyl methacrylate) and Si nanoparticles dissolved in acetone and DMF were injected. After electrospinning process and carbonization, Si/CNFs nanoparticles composite was achieved. The CNFs could diminish the large Si volume expansion and improve the electric conductivity via the formation of continuous electron pathways. In addition, the Si surface in contact with the electrolyte was reduced by the CNFs, thus preventing the Si nanoparticle pulverization during cycling. Hence, the resulted composite showed an outstanding rate and cycling performance. At the rate of 3C, the capacity loss was only 1% after 300 cycles. In addition, 52.2% of the original capacity was still retained with the rate increment from 10C to 12 C, which demonstrates good cycle stability and high-rate capability.

In another approach, Chen et al. [141] fabricated a novel nanofiber with hollow core-shell structured silicon@carbon nanoparticles embedded in CNFs (Si@C/CNFs). The composite fabrication process is shown in Fig. 7. The voids between the carbon shell and the Si nanoparticles core allowed the formation of a stable SEI film and aided to accommodate the Si volume changes during the charging-discharging process. Further, both the carbon shell and CNFs offered superior electrical conductivity. A high reversible capacity of 1020.7 mAh/g was delivered by the resulted electrodes at 0.2 A/g after 100 cycles. In addition, at the high current density of 3.2 A/g, these composite electrodes exhibited excellent cycling performance. The other means to composite CNFs materials with Si are branched CNFs on Si nanowires [142], branched CNFs on Si particles [143], and Si nanoparticles anchored onto CNFs [144].

5.1.2. Si-Graphene

Another excellent choice to composite with Si is graphene because of its superior mechanical properties, large theoretical surface area of 2630 m^2/g, and excellent electrical conductivity [145-148]. Si/graphene composites were firstly prepared by Chou et al. [149] via simple manual mixing. However, this approach would result in the weak adhesion between the graphene sheet and Si nanoparticles, and the non-uniform distribution of the Si nanoparticles on the graphene sheets because of the weak interaction and agglomeration [150].

To create well-mixed nanocomposites, electrostatic self-assembly is an effective approach. It is based on the electrostatic attraction between sequentially absorbed components with opposite charges. Graphene oxide displays a negative charge because of the ionization of phenolic hydroxyl and carboxylic acid groups existing on it. Si nanoparticles are easily oxidized to form a surface oxide layer, endowing with a negative charge, and then functionalized to interact with graphene oxide. This leads to the uniform Si/graphene composite [151]. However, the presence of an oxide layer as both a Li^+ diffusion barrier and an electrical insulator negatively affects the Si-based materials' electrochemical performance, including lower Coulombic efficiency and reversible capacity [152-154]. Therefore, the usage of an oxide layer (e.g., SiO_2) can pose a problem. In one approach presented by Zhou et al. [155], Si nanoparticles with a surface oxide layer (SiO_x) were firstly functionalized by polyelectrolyte poly(diallydimethylammonium chloride) (PDDA) with the positive charge and then added into a graphene oxide dispersed aqueous solution. PDDA-functionalized Si nanoparticles were wrapped by graphene oxide via the electrostatic attraction between the graphene

oxide and the PDDA (Fig. 8). After freeze-drying, thermal reduction, and hydrofluoric acid treatment, complete decomposition of PDDA and etching away the SiO_x from the Si nanoparticles occurred. The resulted nanocomposite exhibited excellent rate capability and stable cycling performance (1205 mAh/g after 150 cycles).

Such sandwich structure has been found to play an important role in the enhancement of the Si/graphene composites' performance [156-158]. In this configuration, hierarchically porous structure can be constructed by alternating stacked elastic layers of graphene. This offers a sufficient void space for Si materials' insertion, and the inside void space can accommodate the Si volume changes and buffer the strain during the charging-discharging process. The number and the thickness of layers for this sandwich structure have been shown to have a direct effect on the properties of Coulombic efficiencies, first discharge capacity, and reversible efficiencies of batteries [157].

In another electrostatic approach, acid-treated Si nanoparticles were used instead of Si nanoparticles with an oxide layer to prepare the pyrolyzed polyaniline (PANI)-grafted Si nanoparticles uniformly encapsulated within graphene. In-situ polymerization of aniline initiated on the aniline functionalized-Si nanoparticles formed a PANI layer on the Si surface. Electrostatic attraction and π–π interaction between graphene oxide and PANI resulted in the wrapping of the PANI-grafted Si nanoparticles by the graphene oxide. Finally, PANI and graphene oxide were pyrolyzed (Fig. 9). The Si nanoparticles and graphene sheets were firmly bound together in the composite via this pyrolyzed PANI layer. Relative to physically mixed Si/graphene composites and pure Si nanoparticles, the resulted composite materials showed better Coulombic efficiency and cycling stability. A specific capacity of about 900 mAh/g could be still delivered after 300 cycles at 2 A/g, corresponding to the capacity retention of about 76%. The improved electrochemical performance was related to the better electronic conductivity, the absence of surface oxides, strong interaction between the firmly-bound carbon-coated Si nanoparticles and the graphene sheets, and faster ion diffusion rate [159].

In these composites, the synergistic functions of Si nanoparticles, amorphous carbon, and graphene have been shown to result in the improved electrochemical performance. For example, Yi et al. [160] reported that at the high mass loading, low electrical resistance could be maintained because of the dual conductive networks both between different Si particles created by graphene and within single Si particles created by amorphous carbon in micro-sized Si@carbon-graphene composite. Correspondingly, the obtained electrode showed high Coulombic efficiency (99.51% from 2nd to 100th cycle) and areal capacity (3.2 mAh/cm^2 after 100 cycles). In addition, Agyeman et al. [161] reported the excellent electrochemical properties of reduced graphene oxide/Si@carbon composite with sandwich structure (high gravimetric capacity and long cycle life) and ascribed it to the synergistic effect of the graphene sheet supported sandwich structure, carbon coating, and uniformly distributed Si nanoparticles, maintaining the overall electrode highly conductive, preventing the Si nanoparticle aggregation and pulverization and maintaining the stability of the structure.

In an effort to obtain improved electrochemical performance, Si nanoparticles/graphene composites with core-shell structures have been also proposed. For example, multi-layer graphene was directly grown on the Si nanoparticles' surface by Son et al. [162] via the CVD technique. This was done to receive well cycling performance with considerably greater volumetric energy density. Sliding between adjacent layers of graphene shell could accommodate the volume changes of Si nanoparticles. Besides, in the LIB cell, at the current density of 0.5 C, volumetric energy densities at the first and 200th cycle were 972 and 700 Wh/L respectively, which are 1.8 and 1.5 times greater than those reported for the commercial LIBs (550 Wh/L). In another approach, multi-layer graphene was catalytically grown on the surface of electroless Ni (as the catalyst)-coated Si nanoparticles. By using the composite, reversible discharge capacity retained up to 1909 mAh/g at the current density of 0.2 A/g after 100 cycles. Even at the high current density of 52 A/g, discharge capacity of 975 mAh/g was received. It was suggested that the flexibility and mechanical strength of graphene can mitigate the drastic Si expansion and close contact between the Si nanoparticle and graphene providing high conductivity. In addition, graphene layers prevented direct exposure of Si nanoparticles to the electrolyte, which is useful for maintaining the SEI films' stability [150].

Other Si/carbon composites are summarized in Table 1.

Table 2.
Li storage performance of TMO/CNTs composite materials.

Sample	Structure	Preparation Method	Specific Capacitance	Ref
Co_3O_4/CNT	Co_3O_4 nanocrystals dispersed in the CNTs matrix	hydrothermal method	510 mAh/g after 500 cycles	[203]
Co_3O_4/CNT	Co_3O_4 spheres threaded with CNTs	hydrothermal method	400 mAh/g at 6000 mA/g	[204]
Co-Co_3O_4/CNT	Co or Co3O4 nanoparticles embedded in the CNTs	solvothermal method	600 mAh/g after 120 cycles	[205]
SnO/MWCNT	SnO2 deposited in the interior of MWCNT	diffusion method	505.9 mAh/g after 40 cycles	[206]
SnO_2/MWCNT	mesoporous SnO_2 overlaid on the outside surface of MWCNTs	hydrothermal method	344.5 mA h/g after 50 cycles	[207]
CNT/SnO_2−Au	Au species dispersed over the amorphous SnO_2 overlayers supported on coaxial CNT	one-pot synthetic route	467 mA h/g at.6 A/g	[208]
Ni-NiO-CNT	Ni-NiO particles attached onto CNT	combustion method	736 mAh/g at 200 mA/g after 50 cycles	[209]
NiO/CNTs	porous NiO microspheres interconnected by CNTs	pyrolysis	812 mAh/g at 100 mA/g after 100 cycles	[210]
NiO/MWCNT	NiO particles distributed on the surface of MWCNTs	vacuum solution infiltration method and calcination treatment	873 mAh/g at 0.1 C after 50 cycles	[211]

5.2. TMO-carbon composites

5.2.1. TMO-CNT

Research efforts to improve the chemistry of LIBs have resulted in the emergence of conversion-based electrode materials such as TMO. The following relation can describe the reaction mechanism of this group:

$nLi^+ + ne^- + Mn^+O \leftrightarrow nLiO + M^0$
M= (Mn, Mo, Fe, V, Co, Ti, Cu, etc.)

TMO nanoparticles have shown high recharging rates and electrochemical capacities over 700 mAh/g, with the capacity retention of 100% after 100 cycles [175-179].

Amon different TMOs, the electrochemically active ones including Fe_3O_4, Fe_2O_3, NiO, f, Co_3O_4, and SnO_2 have been considered as potential LIB electrodes due to their high theoretical specific capacities, non-toxicity, and being earth-abundant. For instance, the theoretical capacity of 1007 mAh/g has been received by Fe_2O_3 anodes [180, 181]. Nonetheless, the pulverization of electrode resulted from the volume expansion (over 200%) during the charging-discharging process and poor conductivity cause a drastic capacity fading and hinder the practical application of Fe_2O_3 as LIB anode materials [182]. To address these issues, several strategies have been employed including heteroatom doping [183, 184], nano-crystallization [185], and materials compositing [186, 187]. Combining the carbon materials and nanostructured Fe_2O_3 to fabricate composite structures is a promising approach, creating a synergistic effect on the electrochemical performance of the battery. Fe_2O_3 with a nano-size structure provides a high surface area and short diffusion pathway for Li-ions. The conductive carbon matrix can consolidate the nanocomposites' integrity and also offers fast transfer paths for the electrons [188]. So far, many attempts have been made to increase the electrochemical performance of Fe_2O_3/carbon composites through designing the carbon matrices with various morphologies [189-191]. Because of its superior performance over typical carbon-Fe_2O_3 composite, CNT-Fe_2O_3 composite has lately received more attention. For example, Su et al. [192] synthesized bubble-nanorod-structured Fe_2O_3/CNTs as high-performance LIB anode materials using the electrospinning method. At the current density of 1 A/g, the discharge capacity of the composite was 812 mAh/g after 300 cycles. It was about three times higher than that of hollow bare Fe_2O_3 nanofibers (285 mAh/g). In addition, a composite of Fe_2O_3 nanoparticles firmly anchored onto the surface of CNT was prepared with the specific capacity of 898 mAh/g at the current density of 0.1 A/g after 100 cycles by in-situ regenerating ionic liquid mixture in water [193]. To integrate Fe_2O_3 particles on the hierarchical networks of MWCNTs, the biomimetic strategy was also employed. The resulted composite displayed a high capacity of 822 mAh/g at the current density of 0.05 A/g [194]. The above-mentioned synthesis routes are difficult to implement because they consume a lot of energy and leave chemical residues. In-situ oxidation of residual Fe particles on the CNTs, which is considered a low-cost and environment-friendly method, was shown to be effective in the preparation of high-performance anodes for LIBs [180]. For example, Zhou et al. [195] prepared nanosized Fe_2O_3 decorated SWCNT composite by oxidizing a flow-assembled membrane of Fe/SWCNT. It exhibited great cyclic stability and high reversible capacity (1243 mAh/g).

CNTs have been also employed to fabricate Fe_3O_4/CNTs composites, which improves the electrochemical properties of Fe_2O_3. In this regard, CNTs-Fe_3O_4 nanocomposites synthesized through an inorganic hydrothermal strategy showed a reversible discharge capacity of about

Table 3.
Li storage performance of different metal sulfide-carbon composite materials.

Sample	Structure	Preparation Method	Specific Capacitance	Ref.
MoS_2/carbon	Carbon-coated MoS2 nanorods	Sulfidation and CVD	621 mAh/g at 200 mA/g after 80 cycles	[226]
MoS_2/carbon	MoS_2 nanosheet dispersed in the amorphous carbon	Hydrothermal method	1011 mAh/g after 120 cycles	[227]
MoS_2/ carbon	3D nanoporous architecture	Instant gelation	410 mAh/g at a current density of 1 A/g	[228]
MoS_2/CNT	MoS_2 nanosheets (NSs) on the CNT backbone	Glucose-assisted hydrothermal method	698 mAh/g after 60 cycles	[229]
MoS_2/CNT	layered MoS_2 nanosheets supported on coaxial CNTs	L-cysteine-assisted hydrothermal route	823.4 mAh/g at 100 mA/g after 30 cycles	[230]
MoS_2/graphene	nanosheet—nanosheet	lithiation-assisted exfoliation process and hydrazine vapor reduction technique	915 mAh/g at 0.5 A/g after 700 cycles	[231]
MoS_2/nitrogen-doped graphene	nanosheet	modified Hummers' and Solvothermal methods	1285 mAh/g at 100 mA/g after 50 cycles	[232]
SnS_2/carbon	Carbon-coated SnS_2 nano particles	Solvothermal method	668 mAh/g after 50 cycles	[233]
SnS_2/MWCNT	SnS_2 nanoflakes decorated MWCNTs	Solution-phase approach	510 mAh/g after 30 cycles	[234]
SnS_2/MWCNT	3D hierarchical self-supported 1D/2D hetero-nanostructure	Two subsequent vapor-phase transport method	432 mAh/g at 645 mA/g after 100 cycles	[235]
SnS_2/graphene	SnS2 nanoplate incorporated with graphene nanosheets	solution-based and solid-gas reactions	650 mAh/g at 0.1 A/g after 30 cycles	[236]
SnS_2/graphene	few-layer SnS_2 supports on graphene surface	solution-phase method	920 mAh/g at 100 mA/g after 50 cycles	[237]
VS_4/graphene oxide	single-crystalline VS4 nanostructures distributed on rGO	hydrothermal method	954 mA h/g at 0.1 C after 100 cycles	[238]
VO_x/VN-carbon	VO_x/VN encapsulated in an amorphous carbon matrix	Calcination	380 mAh/g at 500 mA/g after 200 cycles	[239]

700 mA h/g after 50 cycles at 50 mA/g. It was ~ 4 times greater than that of micro-sized Fe_2O_3 (171 mA h/g) [196]. Despite enhancement in the electrochemical performance of Fe_3O_4, the synthesis of Fe_3O_4/CNTs nanocomposites has some limitations including low loading of Fe_3O_4 on the CNTs and poor adhesion of Fe_3O_4 to the CNTs. To modify MWCNTs, Polyvinyl alcohol was employed as a hydrogen bond functionalizing agent. Fe^{3+} and Fe^{2+} were chemically coprecipitated in an alkaline solution in the presence of CNTs, forming Fe_3O_4 nanoparticles along the sidewalls of the functionalized-CNTs. High discharge capacity (656 mAh/g after 145 cycles) with stable cyclic retention was delivered by CNTs–66.7 wt.% Fe_3O_4 nanocomposite [197].

As mentioned above, MnO_2 with the theoretical capacity of 1250 mAh/g is the other promising LIB anode material. However, some drawbacks limit its application. The poor electronic conductivity results in the low Coulombic efficiency and inferior rate capability, and large volume changes during the phase conversion reaction lead to the poor cycling stability [198, 199]. To enhance its electrochemical properties, surface modification of MnO_2 via the carbon coating such as CNTs is proved to be effective not only in improving the structural stability and electrical contact during cycling but also in mitigating the typical agglomeration problems accompanied by the nanoparticles and some side reactions between the electrolyte and the electrode [200]. However, a complete coating method is usually expensive and difficult. In addition, during lithiation/delithiation, the contraction/expansion of the TMOs can break the coating. To address these limitations, Mao et al. [201] proposed an inner coating method using CNTs to form a 3D mechanical and electronic conductive network. It increased the reactive area, improved the ionic and electronic conductivity, and accommodated the MnO_2 volume changes. The reversible capacity of MnO_2/CNT (with inner coating) composite was 1097.3 mAh/g which was higher than that of MnO_2 (without inner coating, 528.0 mAh /g). Inner coating approach also improved cycling stability. In another approach, Fan et al. [202] used atomic layer deposition to apply aluminum oxide film with ultrathin thickness onto the MnO_2/CNT composite. The non-reactive Al_2O_3 layer restrained the volume change strain of MnO_2. In addition, it offered a stable film to protect MnO_2 and CNTs from the unpleasant reactions with the electrolyte. Depending on the coating thickness, the Coulombic efficiency of the electrodes at the first cycle was enhanced to different extents. In the following cycles, good ability of capacity retention, high specific capacity, and perfect rate charge/discharge performance were provided by the coated electrodes. Other TMO/CNT composites are summarized in Table 2.

5.2.2. TMO-Graphene

CoO has received a lot of attention due to its simple synthesis process and high specific capacity (715 mAh/g). [212]. However, CoO nanoparticles have poor durability, insufficient conductivity, and a small specific surface area. To address these drawbacks, carbon composite materials with excellent durability and significant conductivity are commonly employed to support CoO nanoparticles [213-215]. In this regard, Zhou et al. [216] used a hydrothermal reaction and annealing process to synthesize the nanoporous CoO nanowire clusters on a 3D porous cloth of graphene. The unique microstructures of the composite components not only improved ionic and electronic conductivity but also significantly suppressed the volume changes during the charge-discharge cycles. Accordingly, the resulted composite showed excellent rate performance, good stability, and high specific capacity. In another research, wrapping of hierarchical CoO nanospheres with graphene via the hydrothermal treatment and vulcanization resulted in considerably better cycle stability and Li storage performance than the single CoO electrode. At the current density of 100 mA/g, the initial discharge capacity of the composite was 1974 mAh/g [217]. Tan et al. [218] employed a simple hydrothermal method to synthesize the conversion Co_3O_4/Graphene composite. Outstanding extreme-temperature Li storage capacity was provided by this composite. This makes it a viable LIB anode material. Thanks to the high conductivity of graphene, excellent lithiation/delithiation potential of Co_3O_4, and the ingenious nanostructure, the Co_3O_4/graphene anode had a higher temperature than the alloy and intercalation anodes at the temperatures below zero. NiO and TiO_2 are the other TMOs which has been investigated to composite with graphene, used as anode materials. For instance, Fu et al. [219] fabricated a unique 3D hierarchically porous NiO micro-flowers/graphene paper electrode. 3D porous structure combined the advantages of both micro-sized NiO flowers and graphene. Hierarchical between-layer pores were induced by the micro-sized NiO flowers which improved the electrolyte penetration and prevented the graphene layers from re-stacking. Highly flexible and conductive graphene buffered the NiO volume expansion during the charging/discharging process and provided rapid ions/electrons transfer. Deng et al. [220] synthesized TiO_2/graphene nanosheet composite with 3D structure via an in-situ method. The porous honeycomb structure had high stability and abundant Li/electron pathways. It, as LIB anode, showed outstanding rate and cycle performance. At the current density of 16.5 A/g, the capacity of 184 mAh/g was maintained after 10000 cycles. At the current density of 52.5 A/g, the electrode could still receive the reversible capacity of above 125 mAh/g.

The mixed TMOs composited with graphene have been also studied as the LIB electrodes. In this regard, Gong et al. [221] synthesized $Co_2V_2O_7$/graphene composite via a simple water bath and used it as LIB anode. In this composite, $Co_2V_2O_7$ microplatelets with the hexagonal structure were uniformly attached to the few-layer graphene. The obtained composite showed a high reversible capacity of 1048 mAh/g after 300 cycles at 1 A/g and excellent rate capability. This resulted from the synergistic effects of $Co_2V_2O_7$ and graphene. Shen et al. [222] prepared SnO_2/$NiFe_2O_4$/Graphene nanocomposites via a one-step hydrothermal synthesis technique. These nanocomposites provided good rate performance and cycle stability. The excellent anode performance was ascribed to the synergetic effect between the graphene slices and the SnO_2 nanoparticle. The graphene nanosheets increased the specific surface area and reduced the electrical resistance. Meantime, SnO_2 participated in the electrochemical reaction and acted as a buffer in the system. To achieve ultrafast Li-ion storage performance, Lin et al. [223] suggested a synergistic combination of a highly conductive vertical graphene framework and nitrogen-doped $Li_4Ti_5O_{12}$ nanoparticles. Significant advantages such as great structural stability, enhanced electrical conductivity, and high specific surface area were achieved owning to the positive synergistic effect of vertical graphene backbone with high conductivity and nitrogen doping. Accordingly, long-term cycle stability (98.9% capacity retention after 10000 cycles) and high-rate capacity of 142.5 mAh/g at 20 °C were received.

In addition to above-mentioned composites,, metal-organic framework (MOF) composites have also great potential application prospects in the field of LIBs [224]. In this regard, Ni-based MOF hollow microspheres were grown on a substrate of graphene foam via a simple solvothermal method. The obtained composite, as an independent LIB anode, showed superior cycle stability and specific capacity to graphene foam and pure NiO. The great electrochemical performance was ascribed to the synergistic effect between the graphene foam and NiO components. The GF matrix increased the electrode's conductivity. It also provided a versatile platform for the active elements loading, hindering NiO from escaping and diffusing into the solution during cycling. Meantime, the volume expansion of metal oxide was effectively reduced by the layered hollow structure of NiO [225].

5.3. Other carbon composites

Research in the field of LIB composite anodes is not limited to the carbon-silicon and carbon-transition metal oxides materials. Other composites used and their Li storage performance are shown in Table 3.

6. Summary and outlook

This paper reviews the application of carbon-based materials and their composites as potential LIB anode materials. According to the literature review, carbonaceous materials are prospective substances which could be used effectively as anodes for Li-ion battery applications. However, the current commercial graphite anodes used in LIBs have a low theoretical capacity and serious safety issues. Carbon nanostructures including graphene, CNTs, and CNFs with short ion diffusion length and high available surface areas have been shown to provide better electrochemical performance over the commercial LIB anode materials. In addition, their capacity and rate capability can be further enhanced by accurate structural engineering. For example, to meet the requirements needed for high energy/power electrochemical cells, carbon nanostructures can combine with alloy or metal oxide anodes to form carbon-based nanocomposites with improved electrochemical performance in a synergistic way. In spite of great advancement in carbon nanostructures as LIB anodes, there are some questions and challenges facing their development for practical usage. First, the lithiation/delithiation mechanism of carbon-based nanocomposites should be understood in-depth to obtain valuable data for their designing and optimizing. Second, over the first charge/discharge cycles, these nanocomposites commonly show large irreversible capacity which is mainly resulted from excessive SEI formation during discharging. To mitigate this challenge, further efforts like designing an artificial SEI layer, prelithiation treatment, etc. are needed. Third, developing novel polymer binders and electrolyte additives is needed to enhance electrode performance. In fact, the integrity of electrodes, as well as the adhesion between the active materials and current collectors, can be affected by binders, while the formation of a stable and thin SEI layer can be facilitated by electrolyte additives, which contributes to the charge efficiency and cycling stability of LIBs cells. Last, the synthesis process should be adapted and simplified for industrial requirements. Hence, future attempts need to be focused on comprehensive research into the in-depth understanding of the relation between electrochemical performance and composite structure as well as structural design to develop low cost-high potential nanocarbon-based anode materials.

REFERENCES

[1] V.K.H. Bui, M.K. Kumar, M. Alinaghibeigi, S. Moolayadukkam, S. Eskandarinejad, S. Mahmoudi, S. Mirzamohammadi, M. Rezaei-khamseh, A review on zinc oxide composites for energy storage applications: solar cells, batteries, and supercapacitors, Journal of Composites and Compounds 3(8) (2021) 182-193.
[2] P. Roy, S.K.J.J.o.M.C.A. Srivastava, Nanostructured anode materials for lithium ion batteries, 3(6) (2015) 2454-2484.
[3] F. Sharifianjazi, A. Esmaeilkhanian, L. Bazli, S. Eskandarinezhad, S. Khaksar, P. Shafiee, M. Yusuf, B. Abdullah, P. Salahshour, F. Sadeghi, A review on recent advances in dry reforming of methane over Ni-and Co-based nanocatalysts, International Journal of Hydrogen Energy (2021).
[4] N. Aboualigaledari, M.J.J.o.C. Rahmani, Compounds, A review on the synthesis of the TiO_2-based photocatalyst for the environmental purification, 3(6) (2021) 25-42.
[5] L. Li, D. Zhang, J. Deng, Y. Gou, J. Fang, H. Cui, Y. Zhao, M.J.C. Cao, Carbon-based materials for fast charging lithium-ion batteries, 183 (2021) 721-734.
[6] L.S. Fard, N.S. Peighambardoust, H.W. Jang, A. Dehghan, N.N.K. Saligheh, M. Iranpour, M.I. Rajabi, The rechargeable aluminum-ion battery with different composite cathodes: A review, Journal of Composites and Compounds 2(4) (2020) 138-146.
[7] M. Armand, J.-M.J.n. Tarascon, Building better batteries, 451(7179) (2008) 652-657.
[8] B. Scrosati, J.J.J.o.p.s. Garche, Lithium batteries: Status, prospects and future, 195(9) (2010) 2419-2430.
[9] J.-M. Tarascon, M. Armand, Issues and challenges facing rechargeable lithium batteries, Materials for sustainable energy: a collection of peer-reviewed research and review articles from Nature Publishing Group, World Scientific2011, pp. 171-179.
[10] X.-M. Liu, Z. dong Huang, S. woon Oh, B. Zhang, P.-C. Ma, M.M. Yuen, J.-K.J.C.S. Kim, Technology, Carbon nanotube (CNT)-based composites as electrode material for rechargeable Li-ion batteries: a review, 72(2) (2012) 121-144.
[11] W.-J.J.J.o.P.S. Zhang, A review of the electrochemical performance of alloy anodes for lithium-ion batteries, 196(1) (2011) 13-24.
[12] K.J.T.j.o.p.c.l. Abraham, Prospects and limits of energy storage in batteries, 6(5) (2015) 830-844.
[13] H. Cheng, J.G. Shapter, Y. Li, G.J.J.o.E.C. Gao, Recent progress of advanced anode materials of lithium-ion batteries, 57 (2021) 451-468.
[14] R. Li, S. Nie, C. Miao, Y. Xin, H. Mou, G. Xu, W.J.J.o.C. Xiao, I. Science, Heterostructural Sn/SnO_2 microcube powders coated by a nitrogen-doped carbon layer as good-performance anode materials for lithium ion batteries, 606 (2022) 1042-1054.
[15] M.M. Obeid, Q.J.C. Sun, Assembling biphenylene into 3D porous metallic carbon allotrope for promising anode of lithium-ion batteries, 188 (2022) 95-103.
[16] F. Yao, D.T. Pham, Y.H.J.C. Lee, Carbon-based materials for lithium-ion batteries, electrochemical capacitors, and their hybrid devices, 8(14) (2015) 2284-2311.
[17] S. Goriparti, E. Miele, F. De Angelis, E. Di Fabrizio, R.P. Zaccaria, C.J.J.o.p.s. Capiglia, Review on recent progress of nanostructured anode materials for Li-ion batteries, 257 (2014) 421-443.
[18] N. Mahmood, T. Tang, Y.J.A.E.M. Hou, Nanostructured anode materials for lithium ion batteries: progress, challenge and perspective, 6(17) (2016) 1600374.
[19] X. Zuo, J. Zhu, P. Müller-Buschbaum, Y.-J.J.N.E. Cheng, Silicon based lithium-ion battery anodes: A chronicle perspective review, 31 (2017) 113-143.
[20] Y. Wu, J. Wang, K. Jiang, S.J.F.o.P. Fan, Applications of carbon nanotubes in high performance lithium ion batteries, 9(3) (2014) 351-369.
[21] C. De las Casas, W.J.J.o.P.S. Li, A review of application of carbon nanotubes for lithium ion battery anode material, 208 (2012) 74-85.
[22] J. Lu, Z. Chen, F. Pan, Y. Cui, K.J.E.E.R. Amine, High-performance anode materials for rechargeable lithium-ion batteries, 1(1) (2018) 35-53
[23] B. Boukamp, G. Lesh, R.J.J.o.t.E.S. Huggins, All-solid lithium electrodes with mixed-conductor matrix, 128(4) (1981) 725.
[24] B. Liang, Y. Liu, Y.J.J.o.P.s. Xu, Silicon-based materials as high capacity anodes for next generation lithium ion batteries, 267 (2014) 469-490.
[25] H. Wu, Y.J.N.t. Cui, Designing nanostructured Si anodes for high energy lithium ion batteries, 7(5) (2012) 414-429.
[26] Y. Oumellal, N. Delpuech, D. Mazouzi, N. Dupre, J. Gaubicher, P. Moreau, P. Soudan, B. Lestriez, D.J.J.o.M.C. Guyomard, The failure mechanism of nano-sized Si-based negative electrodes for lithium ion batteries, 21(17) (2011) 6201-6208.
[27] C.K. Chan, R. Ruffo, S.S. Hong, Y.J.J.o.P.S. Cui, Surface chemistry and morphology of the solid electrolyte interphase on silicon nanowire lithium-ion battery anodes, 189(2) (2009) 1132-1140.
[28] S.H. Ng, J. Wang, D. Wexler, K. Konstantinov, Z.P. Guo, H.K.J.A.C.I.E. Liu, Highly reversible lithium storage in spheroidal carbon-coated silicon nanocomposites as anodes for lithium-ion batteries, 45(41) (2006) 6896-6899.
[29] M.A. Rahman, G. Song, A.I. Bhatt, Y.C. Wong, C.J.A.F.M. Wen, Nanostructured silicon anodes for high-performance lithium-ion batteries, 26(5) (2016) 647-678.
[30] J.H. Ryu, J.W. Kim, Y.-E. Sung, S.M.J.E. Oh, s.-s. letters, Failure modes of silicon powder negative electrode in lithium secondary batteries, 7(10) (2004) A306.
[31] L. Beaulieu, K. Eberman, R. Turner, L. Krause, J.J.E. Dahn, S.-S. Letters, Colossal reversible volume changes in lithium alloys, 4(9) (2001) A137.
[32] H. Chen, Z. Wu, Z. Su, S. Chen, C. Yan, M. Al-Mamun, Y. Tang, S.J.N.E. Zhang, A mechanically robust self-healing binder for silicon anode in lithium ion batteries, 81 (2021) 105654.
[33] M. Ashuri, Q. He, L.L.J.N. Shaw, Silicon as a potential anode material for Li-ion batteries: where size, geometry and structure matter, 8(1) (2016) 74-103.
[34] M.D. Bhatt, J.Y.J.I.J.o.H.E. Lee, High capacity conversion anodes in Li-ion batteries: A review, 44(21) (2019) 10852-10905.
[35] L. Bazli, M. Siavashi, A. Shiravi, A review of carbon nanotube/TiO_2 composite prepared via sol-gel method, Journal of Composites and Compounds 1(1) (2019) 1-9.
[36] Y. Zhu, S. Murali, M.D. Stoller, K. Ganesh, W. Cai, P.J. Ferreira, A. Pirkle,

R.M. Wallace, K.A. Cychosz, M.J.s. Thommes, Carbon-based supercapacitors produced by activation of graphene, 332(6037) (2011) 1537-1541.
[37] G. Wang, H. Wang, X. Lu, Y. Ling, M. Yu, T. Zhai, Y. Tong, Y.J.A.m. Li, Solid-state supercapacitor based on activated carbon cloths exhibits excellent rate capability, 26(17) (2014) 2676-2682.
[38] S. Korkmaz, İ.A. Kariper, O. Karaman, C.J.C.I. Karaman, The production of rGO/RuO_2 aerogel supercapacitor and analysis of its electrochemical performances, 47(24) (2021) 34514-34520.
[39] M.K. Zadeh, M. Yeganeh, M.T. Shoushtari, A.J.S.M. Esmaeilkhanian, Corrosion performance of polypyrrole-coated metals: A review of perspectives and recent advances, 274 (2021) 116723.
[40] Q. Wang, H. Li, L. Chen, X.J.S.S.I. Huang, Novel spherical microporous carbon as anode material for Li-ion batteries, 152 (2002) 43-50.
[41] B.J. Landi, M.J. Ganter, C.D. Cress, R.A. DiLeo, R.P.J.E. Raffaelle, E. Science, Carbon nanotubes for lithium ion batteries, 2(6) (2009) 638-654.
[42] M. Endo, C. Kim, K. Nishimura, T. Fujino, K.J.C. Miyashita, Recent development of carbon materials for Li ion batteries, 38(2) (2000) 183-197.
[43] Z.-Z. Jiang, Z.-B. Wang, Y.-Y. Chu, D.-M. Gu, G.-P.J.E. Yin, E. Science, Ultrahigh stable carbon riveted Pt/TiO 2–C catalyst prepared by in situ carbonized glucose for proton exchange membrane fuel cell, 4(3) (2011) 728-735.
[44] J.E. Mink, J.P. Rojas, B.E. Logan, M.M.J.N.L. Hussain, Vertically grown multiwalled carbon nanotube anode and nickel silicide integrated high performance microsized (1.25 μL) microbial fuel cell, 12(2) (2012) 791-795.
[45] H. Karimi-Maleh, İ.A. Kariper, C. Karaman, S. Korkmaz, O.J.F. Karaman, Direct utilization of radioactive irradiated graphite as a high-energy supercapacitor a promising electrode material, 325 (2022) 124843.
[46] A. Esmaeilkhanian, F. Sharifianjazi, N. Parvin, M.A.J.J.o.P.D.A.P. Kooti, Cytotoxicity of thermoresponsive core/shell Ni x $Co_{1-x}Fe_2O_4$/PEG nanoparticles synthesized by the sol–gel method, Journal of Physics D: Applied Physics, 54(29) (2021) 295002.
[47] H. Karimi-Maleh, C. Karaman, O. Karaman, F. Karimi, Y. Vasseghian, L. Fu, M. Baghayeri, J. Rouhi, P. Senthil Kumar, P.-L.J.J.o.N.i.C. Show, Nanochemistry approach for the fabrication of Fe and N co-decorated biomass-derived activated carbon frameworks: a promising oxygen reduction reaction electrocatalyst in neutral media, (2022) 1-11.
[48] C. Karaman, O. Karaman, P.-L. Show, H. Karimi-Maleh, N.J.C. Zare, Congo red dye removal from aqueous environment by cationic surfactant modified-biomass derived carbon: equilibrium, kinetic, and thermodynamic modeling, and forecasting via artificial neural network approach, 290 (2022) 133346.
[49] H. Li, H.J.C.C. Zhou, Enhancing the performances of Li-ion batteries by carbon-coating: present and future, 48(9) (2012) 1201-1217.
[50] G.-A. Nazri, G. Pistoia, Lithium batteries: science and technology, Springer Science & Business Media2008.
[51] R. Marom, S.F. Amalraj, N. Leifer, D. Jacob, D.J.J.o.M.C. Aurbach, A review of advanced and practical lithium battery materials, 21(27) (2011) 9938-9954.
[52] Z. Jian, Z. Xing, C. Bommier, Z. Li, X.J.A.E.M. Ji, Hard carbon microspheres: potassium-ion anode versus sodium-ion anode, 6(3) (2016) 1501874.
[53] R.A. Adams, A. Varma, V.G.J.A.E.M. Pol, Carbon anodes for nonaqueous alkali metal-ion batteries and their thermal safety aspects, 9(35) (2019) 1900550.
[54] S. Huang, Z. Li, B. Wang, J. Zhang, Z. Peng, R. Qi, J. Wang, Y.J.A.F.M. Zhao, N-Doping and defective nanographitic domain coupled hard carbon nanoshells for high performance lithium/sodium storage, 28(10) (2018) 1706294.
[55] F.A. Soto, P. Yan, M.H. Engelhard, A. Marzouk, C. Wang, G. Xu, Z. Chen, K. Amine, J. Liu, V.L.J.A.m. Sprenkle, Tuning the solid electrolyte interphase for selective Li-and Na-ion storage in hard carbon, 29(18) (2017) 1606860.
[56] H. Li, Z. Wang, L. Chen, X.J.A.m. Huang, Research on advanced materials for Li-ion batteries, 21(45) (2009) 4593-4607
[57] Y. Li, R.A. Adams, A. Arora, V.G. Pol, A.M. Levine, R.J. Lee, K. Akato, A.K. Naskar, M.P.J.J.o.T.E.S. Paranthaman, Sustainable potassium-ion battery anodes derived from waste-tire rubber, 164(6) (2017) A1234.
[58] X. Zhao, Y. Ding, Q. Xu, X. Yu, Y. Liu, H.J.A.E.M. Shen, Low-Temperature Growth of Hard Carbon with Graphite Crystal for Sodium-Ion Storage with High Initial Coulombic Efficiency: A General Method, 9(10) (2019) 1803648.
[59] Y. Wang, Y. Li, S.S. Mao, D. Ye, W. Liu, R. Guo, Z. Feng, J. Kong, J.J.S.e. Xie, fuels, N-doped porous hard-carbon derived from recycled separators for efficient lithium-ion and sodium-ion batteries, 3(3) (2019) 717-722.
[60] L.F. Zhao, Z. Hu, W.H. Lai, Y. Tao, J. Peng, Z.C. Miao, Y.X. Wang, S.L. Chou, H.K. Liu, S.X.J.A.E.M. Dou, Hard carbon anodes: fundamental understanding and commercial perspectives for Na-ion batteries beyond Li-ion and K-ion counterparts, 11(1) (2021) 2002704.
[61] X. Wu, Y. Chen, Z. Xing, C.W.K. Lam, S.S. Pang, W. Zhang, Z.J.A.E.M. Ju, Advanced carbon-based anodes for potassium-ion batteries, 9(21) (2019) 1900343.
[62] S. Alvin, H.S. Cahyadi, J. Hwang, W. Chang, S.K. Kwak, J.J.A.E.M. Kim, Revealing the intercalation mechanisms of lithium, sodium, and potassium in hard carbon, 10(20) (2020) 2000283.
[63] J. Dahn, W. Xing, Y.J.C. Gao, The “falling cards model” for the structure of microporous carbons, 35(6) (1997) 825-830.
[64] L. Xie, C. Tang, Z. Bi, M. Song, Y. Fan, C. Yan, X. Li, F. Su, Q. Zhang, C.J.A.E.M. Chen, Hard Carbon Anodes for Next-Generation Li-Ion Batteries: Review and Perspective, 11(38) (2021) 2101650.
[65] C.A. Bridges, X.-G. Sun, J. Zhao, M.P. Paranthaman, S.J.T.J.o.P.C.C. Dai, In situ observation of solid electrolyte interphase formation in ordered mesoporous hard carbon by small-angle neutron scattering, 116(14) (2012) 7701-7711.
[66] P.J.J.J.o.M.S. Harris, Fullerene-like models for microporous carbon, 48(2) (2013) 565-577.
[67] Z. Zhou, Z. Gu, Y. He, D. Peng, C. Bao, H.J.I.J.E.S. Liu, Controlling the Structure and Electrochemical Properties of Anode Prepared from Phenolic Resin for Li-ion Batteries, 14 (2019) 6976-6985.
[68] H. Lu, F. Ai, Y. Jia, C. Tang, X. Zhang, Y. Huang, H. Yang, Y.J.S. Cao, Exploring Sodium-Ion Storage Mechanism in Hard Carbons with Different Microstructure Prepared by Ball-Milling Method, 14(39) (2018) 1802694.
[69] Y.-F. Du, G.-H. Sun, Y. Li, J.-Y. Cheng, J.-P. Chen, G. Song, Q.-Q. Kong, L.-J. Xie, C.-M.J.C. Chen, Pre-oxidation of lignin precursors for hard carbon anode with boosted lithium-ion storage capacity, 178 (2021) 243-255.
[70] A. Agrawal, K. Biswas, S. Srivastava, S.J.J.o.S.S.E. Ghosh, Effect of N-doping on hard carbon nano-balls as anode for Li-ion battery: improved hydrothermal synthesis and volume expansion study, 22(11) (2018) 3443-3455.
[71] R. Li, J. Huang, J. Li, L. Cao, X. Zhong, A. Yu, G.J.J.o.E.C. Lu, Nitrogen-doped porous hard carbons derived from shaddock peel for high-capacity lithium-ion battery anodes, 862 (2020) 114044.
[72] Y. Qian, S. Jiang, Y. Li, Z. Yi, J. Zhou, T. Li, Y. Han, Y. Wang, J. Tian, N.J.A.E.M. Lin, In Situ Revealing the Electroactivity of P-O and P-C Bonds in Hard Carbon for High-Capacity and Long-Life Li/K-Ion Batteries, 9(34) (2019) 1901676.
[73] V.P.S. Sidhu, R. Borges, M. Yusuf, S. Mahmoudi, S.F. Ghorbani, M. Hosseinikia, P. Salahshour, F. Sadeghi, M.J.J.o.C. Arefian, Compounds, A comprehensive review of bioactive glass: synthesis, ion substitution, application, challenges, and future perspectives, 3(9) (2021) 247-261.
[74] D. Stevens, J.J.J.o.T.E.S. Dahn, The mechanisms of lithium and sodium insertion in carbon materials, 148(8) (2001) A803.
[75] J.R. Dahn, T. Zheng, Y. Liu, J.J.S. Xue, Mechanisms for lithium insertion in carbonaceous materials, 270(5236) (1995) 590-593.
[76] J. Wang, J.-L. Liu, Y.-G. Wang, C.-X. Wang, Y.-Y.J.E.a. Xia, Pitch modified hard carbons as negative materials for lithium-ion batteries, 74 (2012) 1-7.
[77] H. Fujimoto, K. Tokumitsu, A. Mabuchi, N. Chinnasamy, T.J.J.o.P.S. Kasuh, The anode performance of the hard carbon for the lithium ion battery derived from the oxygen-containing aromatic precursors, 195(21) (2010) 7452-7456.
[78] J. Hu, H. Li, X.J.S.S.I. Huang, Influence of micropore structure on Li-storage capacity in hard carbon spherules, 176(11-12) (2005) 1151-1159.
[79] W. Li, M. Chen, C.J.M.L. Wang, Spherical hard carbon prepared from potato starch using as anode material for Li-ion batteries, 65(23-24) (2011) 3368-3370.
[80] J. Yang, X.-y. Zhou, J. Li, Y.-l. Zou, J.-j.J.M.C. Tang, Physics, Study of nano-porous hard carbons as anode materials for lithium ion batteries, 135(2-3) (2012) 445-450.
[81] I. Tajzad, E. Ghasali, Production methods of CNT-reinforced Al matrix composites: a review, Journal of Composites and Compounds 2(2) (2020) 1-9.
[82] M.F. Heragh, S. Eskandarinezhad, A. Dehghan, Ni-Cu matrix composite reinforced with CNTs: preparation, characterization, wear and corrosion behavior, inhibitory effects, Journal of Composites and Compounds 2(4) (2020) 123-128.
[83] J. Zhao, A. Buldum, J. Han, J.P.J.P.r.l. Lu, First-principles study of Li-intercalated carbon nanotube ropes, 85(8) (2000) 1706.
[84] T. Kar, J. Pattanayak, S.J.T.J.o.P.C.A. Scheiner, Insertion of lithium ions into carbon nanotubes: an ab initio study, 105(45) (2001) 10397-10403.
[85] S. Yang, H. Song, X. Chen, A. Okotrub, L.J.E.a. Bulusheva, Electrochemical performance of arc-produced carbon nanotubes as anode material for lithium-ion batteries, 52(16) (2007) 5286-5293.
[86] H. Shimoda, B. Gao, X. Tang, A. Kleinhammes, L. Fleming, Y. Wu, O.J.P.r.l. Zhou, Lithium intercalation into opened single-wall carbon nanotubes: storage capacity and electronic properties, 88(1) (2001) 015502.
[87] B. Gao, C. Bower, J. Lorentzen, L. Fleming, A. Kleinhammes, X. Tang, L. McNeil, Y. Wu, O.J.C.P.L. Zhou, Enhanced saturation lithium composition in ball-milled single-walled carbon nanotubes, 327(1-2) (2000) 69-75.
[88] C. Garau, A. Frontera, D. Quiñonero, A. Costa, P. Ballester, P.M.J.C.p. Deyà, Ab initio investigations of lithium diffusion in single-walled carbon nanotubes,

297(1-3) (2004) 85-91.
[89] C. Garau, A. Frontera, D. Quiñonero, A. Costa, P. Ballester, P.M.J.C.p.l. Deyà, Lithium diffusion in single-walled carbon nanotubes: a theoretical study, 374(5-6) (2003) 548-555.
[90] K. Nishidate, M.J.P.R.B. Hasegawa, Energetics of lithium ion adsorption on defective carbon nanotubes, 71(24) (2005) 245418.
[91] J. Eom, D. Kim, H.J.J.o.p.s. Kwon, Effects of ball-milling on lithium insertion into multi-walled carbon nanotubes synthesized by thermal chemical vapour deposition, 157(1) (2006) 507-514.
[92] B. Gao, A. Kleinhammes, X. Tang, C. Bower, L. Fleming, Y. Wu, O.J.C.p.l. Zhou, Electrochemical intercalation of single-walled carbon nanotubes with lithium, 307(3-4) (1999) 153-157.
[93] T.P. Kumar, R. Ramesh, Y. Lin, G.T.-K.J.E.C. Fey, Tin-filled carbon nanotubes as insertion anode materials for lithium-ion batteries, 6(6) (2004) 520-525.
[94] V. Meunier, J. Kephart, C. Roland, J.J.P.r.l. Bernholc, Ab initio investigations of lithium diffusion in carbon nanotube systems, 88(7) (2002) 075506.
[95] S. Yang, J. Huo, H. Song, X.J.E.A. Chen, A comparative study of electrochemical properties of two kinds of carbon nanotubes as anode materials for lithium ion batteries, 53(5) (2008) 2238-2244.
[96] X. Huang, X. Qi, F. Boey, H.J.C.S.R. Zhang, Graphene-based composites, 41(2) (2012) 666-686.
[97] J. Hou, Y. Shao, M.W. Ellis, R.B. Moore, B.J.P.C.C.P. Yi, Graphene-based electrochemical energy conversion and storage: fuel cells, supercapacitors and lithium ion batteries, 13(34) (2011) 15384-15402.
[98] F. Niazvand, P.R. Wagh, E. Khazraei, M.B. Dastjerdi, C. Patil, I.A. Najar, Application of carbon allotropes composites for targeted cancer therapy drugs: A review, Journal of Composites and Compounds 3(7) (2021) 140-151.
[99] A. Kazemzadeh, M.A. Meshkat, H. Kazemzadeh, M. Moradi, R. Bahrami, R. Pouriamanesh, Preparation of graphene nanolayers through surfactant-assisted pure shear milling method, Journal of Composites and Compounds 1(1) (2019) 22-26.
[100] F. Sharifianjazi, A.J. Rad, A. Esmaeilkhanian, F. Niazvand, A. Bakhtiari, L. Bazli, M. Abniki, M. Irani, A. Moghanian, Biosensors and nanotechnology for cancer diagnosis (lung and bronchus, breast, prostate, and colon): A systematic review, Biomedical Materials (2021) .
[101] F.S. Moghanlou, M. Vajdi, H. Jafarzadeh, Z. Ahmadi, A. Motallebzadeh, F. Sharifianjazi, M.S. Asl, M. Mohammadi, Spark plasma sinterability and thermal diffusivity of TiN ceramics with graphene additive, Ceramics International 47(7) (2021) 10057-10062.
[102] H. Aghamohammadi, N. Hassanzadeh, R.J.C.I. Eslami-Farsani, A review study on the recent advances in developing the heteroatom-doped graphene and porous graphene as superior anode materials for Li-ion batteries, 47(16) (2021) 22269-22301.
[103] Y. Liu, V.I. Artyukhov, M. Liu, A.R. Harutyunyan, B.I.J.T.j.o.p.c.l. Yakobson, Feasibility of lithium storage on graphene and its derivatives, 4(10) (2013) 1737-1742.
[104] H.J. Hwang, J. Koo, M. Park, N. Park, Y. Kwon, H.J.T.J.o.P.C.C. Lee, Multilayer graphynes for lithium ion battery anode, 117(14) (2013) 6919-6923.
[105] D. Pan, S. Wang, B. Zhao, M. Wu, H. Zhang, Y. Wang, Z.J.C.o.M. Jiao, Li storage properties of disordered graphene nanosheets, 21(14) (2009) 3136-3142.
[106] J. Liu, Q. Zheng, M.D. Goodman, H. Zhu, J. Kim, N.A. Krueger, H. Ning, X. Huang, J. Liu, M.J.A.M. Terrones, Graphene sandwiched mesostructured Li-ion battery electrodes, 28(35) (2016) 7696-7702.
[107] J. Hassoun, F. Bonaccorso, M. Agostini, M. Angelucci, M.G. Betti, R. Cingolani, M. Gemmi, C. Mariani, S. Panero, V.J.N.l. Pellegrini, An advanced lithium-ion battery based on a graphene anode and a lithium iron phosphate cathode, 14(8) (2014) 4901-4906.
[108] U. Bhattacharjee, S. Bhowmik, S. Ghosh, N. Vangapally, S.K.J.C.E.J. Martha, Boron-doped graphene anode coupled with microporous activated carbon cathode for lithium-ion ultracapacitors, 430 (2022) 132835.
[109] D. Sun, Z. Tan, X. Tian, F. Ke, Y. Wu, J.J.N.R. Zhang, Graphene: A promising candidate for charge regulation in high-performance lithium-ion batteries, 14(12) (2021) 4370-4385.
[110] Z.-L. Wang, D. Xu, H.-G. Wang, Z. Wu, X.-B.J.A.n. Zhang, In situ fabrication of porous graphene electrodes for high-performance energy storage, 7(3) (2013) 2422-2430.
[111] T. Bhardwaj, A. Antic, B. Pavan, V. Barone, B.D.J.J.o.t.A.C.S. Fahlman, Enhanced electrochemical lithium storage by graphene nanoribbons, 132(36) (2010) 12556-12558.
[112] E. Yoo, J. Kim, E. Hosono, H.-s. Zhou, T. Kudo, I.J.N.l. Honma, Large reversible Li storage of graphene nanosheet families for use in rechargeable lithium ion batteries, 8(8) (2008) 2277-2282.
[113] P. Lian, X. Zhu, S. Liang, Z. Li, W. Yang, H.J.E.A. Wang, Large reversible capacity of high quality graphene sheets as an anode material for lithium-ion batteries, 55(12) (2010) 3909-3914.
[114] C. Tang, Q. Zhang, M.Q. Zhao, J.Q. Huang, X.B. Cheng, G.L. Tian, H.J. Peng, F.J.A.M. Wei, Lithium-Sulfur Batteries: Nitrogen-Doped Aligned Carbon Nanotube/Graphene Sandwiches: Facile Catalytic Growth on Bifunctional Natural Catalysts and Their Applications as Scaffolds for High-Rate Lithium-Sulfur Batteries (Adv. Mater. 35/2014), 26(35) (2014) 6199-6199.
[115] M.-S. Balogun, Y. Luo, W. Qiu, P. Liu, Y.J.C. Tong, A review of carbon materials and their composites with alloy metals for sodium ion battery anodes, 98 (2016) 162-178.
[116] S. You, H. Tan, L. Wei, W. Tan, C.J.C.A.E.J. Chao Li, Design Strategies of Si/C Composite Anode for Lithium-Ion Batteries, 27(48) (2021) 12237-12256.
[117] C. Xie, N. Xu, P. Shi, Y. Lv, H.M.K. Sari, J.-w. Shi, W. Xiao, J. Qin, H. Yang, W.J.J.o.C. Li, I. Science, Flexible and Robust Silicon/Carbon Nanotube Anodes Exhibiting High Areal Capacities, (2022).
[118] J. Yu, C. Zhang, W. Wu, Y. Cai, Y.J.A.S.S. Zhang, Nodes-connected silicon-carbon nanofibrous hybrids anodes for lithium-ion batteries, 548 (2021) 148944.
[119] I.Z. González, H.-C. Chiu, R. Gauvin, G.P. Demopoulos, Y.J.M.T.C. Verde-Gómez, Silicon doped carbon nanotubes as high energy anode for lithium-ion batteries, 30 (2022) 103158.
[120] Y. Yan, J. Miao, Z. Yang, F.-X. Xiao, H.B. Yang, B. Liu, Y.J.C.S.R. Yang, Carbon nanotube catalysts: recent advances in synthesis, characterization and applications, 44(10) (2015) 3295-3346.
[121] M. Pagliaro, R. Ciriminna, M. Yusuf, S. Eskandarinezhad, I.A. Wani, M. Ghahremani, Z.R. Nezhad, Application of nanocellulose composites in the environmental engineering as a catalyst, flocculants, and energy storages: A review, Journal of Composites and Compounds 3(7) (2021) 114-128.
[122] Y.-j. Qiao, H. Zhang, Y.-x. Hu, W.-p. Li, W.-j. Liu, H.-m. Shang, M.-z. Qu, G.-c. Peng, Z.-w.J.I.J.o.M. Xie, Metallurgy, Materials, A chain-like compound of Si@ CNT nanostructures and MOF-derived porous carbon as an anode for Li-ion batteries, 28(10) (2021) 1611-1620.
[123] R. Epur, M.K. Datta, P.N.J.E.A. Kumta, Nanoscale engineered electrochemically active silicon–CNT heterostructures-novel anodes for Li-ion application, 85 (2012) 680-684.
[124] I.Z. González, H.-C. Chiu, R. Gauvin, G.P. Demopoulos, Y.V.J.M.T.C. Gómez, Silicon doped carbon nanotubes as high energy anode for lithium-ion batteries, (2022) 103158.
[125] T. Kim, Y. Mo, K. Nahm, S.M.J.J.o.p.s. Oh, Carbon nanotubes (CNTs) as a buffer layer in silicon/CNTs composite electrodes for lithium secondary batteries, 162(2) (2006) 1275-1281.
[126] W. Wang, P.N.J.A.n. Kumta, Nanostructured hybrid silicon/carbon nanotube heterostructures: reversible high-capacity lithium-ion anodes, 4(4) (2010) 2233-2241.
[127] C.-F. Sun, H. Zhu, M. Okada, K. Gaskell, Y. Inoue, L. Hu, Y.J.N.L. Wang, Interfacial oxygen stabilizes composite silicon anodes, 15(1) (2015) 703-708.
[128] J.W. Wang, X.H. Liu, K. Zhao, A. Palmer, E. Patten, D. Burton, S.X. Mao, Z. Suo, J.Y.J.A.n. Huang, Sandwich-lithiation and longitudinal crack in amorphous silicon coated on carbon nanofibers, 6(10) (2012) 9158-9167.
[129] C.-M. Wang, X. Li, Z. Wang, W. Xu, J. Liu, F. Gao, L. Kovarik, J.-G. Zhang, J. Howe, D.J.J.N.l. Burton, In situ TEM investigation of congruent phase transition and structural evolution of nanostructured silicon/carbon anode for lithium ion batteries, 12(3) (2012) 1624-1632.
[130] L.-F. Cui, Y. Yang, C.-M. Hsu, Y.J.N.l. Cui, Carbon− silicon core− shell nanowires as high capacity electrode for lithium ion batteries, 9(9) (2009) 3370-3374.
[131] C. Lu, Y. Fan, H. Li, Y. Yang, B.K. Tay, E. Teo, Q.J.C. Zhang, Core–shell CNT–Ni–Si nanowires as a high performance anode material for lithium ion batteries, 63 (2013) 54-60.
[132] C. Xiang, N. Behabtu, Y. Liu, H.G. Chae, C.C. Young, B. Genorio, D.E. Tsentalovich, C. Zhang, D.V. Kosynkin, J.R.J.A.N. Lomeda, Graphene nanoribbons as an advanced precursor for making carbon fiber, 7(2) (2013) 1628-1637.
[133] X.J.M. Huang, Fabrication and properties of carbon fibers, 2(4) (2009) 2369-2403.
[134] C. Zhang, J. Yan, R. Song, L. Chen, Y.J.J.o.M.S. Liu, Surface porous carbon nanofibers based on coaxial electrospinning with improved mechanical strength and cycle stability for freestanding anode in Li-ion batteries, 56(36) (2021) 19996-20007.
[135] H. Zhou, G. Sun, J. Zhao, J.J.J.o.M.S. Li, Sulfur-induced porous carbon nanofibers composite SiO as bifunctional anode for high-performance Li-ion storage, 57(10) (2022) 5954-5963.

[136] T. Hyeon, S. Han, Y.E. Sung, K.W. Park, Y.W.J.A.C.I.E. Kim, High-performance direct methanol fuel cell electrodes using solid-phase-synthesized carbon nanocoils, 42(36) (2003) 4352-4356.
[137] M. Li, N. Li, W. Shao, C.J.N. Zhou, Synthesis of carbon nanofibers by CVD as a catalyst support material using atomically ordered Ni3C nanoparticles, 27(50) (2016) 505706.
[138] S.-J. Kim, M.-C. Kim, S.-B. Han, G.-H. Lee, H.-S. Choe, S.-H. Moon, D.-H. Kwak, S. Hong, K.-W.J.J.o.I. Park, E. Chemistry, 3-D Si/carbon nanofiber as a binder/current collector-free anode for lithium-ion batteries, 49 (2017) 105-111.
[139] M.-S. Wang, W.-L. Song, J. Wang, L.-Z.J.C. Fan, Highly uniform silicon nanoparticle/porous carbon nanofiber hybrids towards free-standing high-performance anodes for lithium-ion batteries, 82 (2015) 337-345.
[140] T.H. Hwang, Y.M. Lee, B.-S. Kong, J.-S. Seo, J.W.J.N.l. Choi, Electrospun core–shell fibers for robust silicon nanoparticle-based lithium ion battery anodes, 12(2) (2012) 802-807.
[141] Y. Chen, Y. Hu, Z. Shen, R. Chen, X. He, X. Zhang, Y. Li, K.J.J.o.P.S. Wu, Hollow core–shell structured silicon@ carbon nanoparticles embed in carbon nanofibers as binder-free anodes for lithium-ion batteries, 342 (2017) 467-475.
[142] T. Song, D.H. Lee, M.S. Kwon, J.M. Choi, H. Han, S.G. Doo, H. Chang, W.I. Park, W. Sigmund, H.J.J.o.M.C. Kim, Silicon nanowires with a carbon nanofiber branch as lithium-ion anode material, 21(34) (2011) 12619-12621.
[143] S.-M. Jang, J. Miyawaki, M. Tsuji, I. Mochida, S.-H.J.C. Yoon, The preparation of a novel Si–CNF composite as an effective anodic material for lithium–ion batteries, 47(15) (2009) 3383-3391.
[144] L. Ji, X.J.E. Zhang, E. Science, Evaluation of Si/carbon composite nanofiber-based insertion anodes for new-generation rechargeable lithium-ion batteries, 3(1) (2010) 124-129.
[145] D. Ma, Z. Cao, A.J.N.-M.L. Hu, Si-based anode materials for Li-ion batteries: a mini review, 6(4) (2014) 347-358.
[146] P. Sehrawat, A. Shabir, C. Julien, S.J.J.o.P.S. Islam, Recent trends in silicon/graphene nanocomposite anodes for lithium-ion batteries, 501 (2021) 229709.
[147] I. Imae, K. Yukinaga, K. Imato, Y. Ooyama, Y.J.C.I. Kimura, Facile silicon/graphene composite synthesis method for application in lithium-ion batteries, (2022) .
[148] P. Shafiee, M.R. Nafchi, S. Eskandarinezhad, S. Mahmoudi, E.J.S. Ahmadi, Sintering, Sol-gel zinc oxide nanoparticles: advances in synthesis and applications, 1(4) (2021) 242-254.
[149] S.-L. Chou, J.-Z. Wang, M. Choucair, H.-K. Liu, J.A. Stride, S.-X.J.E.C. Dou, Enhanced reversible lithium storage in a nanosize silicon/graphene composite, 12(2) (2010) 303-306.
[150] M.-S. Wang, G.-L. Wang, S. Wang, J. Zhang, J. Wang, W. Zhong, F. Tang, Z.-L. Yang, J. Zheng, X.J.C.E.J. Li, In situ catalytic growth 3D multi-layers graphene sheets coated nano-silicon anode for high performance lithium-ion batteries, 356 (2019) 895-903.
[151] Y. Wen, Y. Zhu, A. Langrock, A. Manivannan, S.H. Ehrman, C.J.S. Wang, Graphene-bonded and-encapsulated Si nanoparticles for lithium ion battery anodes, 9(16) (2013) 2810-2816.
[152] Y.S. Hu, R. Demir-Cakan, M.M. Titirici, J.O. Müller, R. Schlögl, M. Antonietti, J.J.A.C.I.E. Maier, Superior storage performance of a Si@ SiOx/C nanocomposite as anode material for lithium-ion batteries, 47(9) (2008) 1645-1649.
[153] B.-C. Yu, Y. Hwa, C.-M. Park, J.-H. Kim, H.-J.J.R.a. Sohn, Effect of oxide layer thickness to nano–Si anode for Li-ion batteries, 3(24) (2013) 9408-9413.
[154] S. Xun, X. Song, L. Wang, M. Grass, Z. Liu, V. Battaglia, G.J.J.o.T.E.S. Liu, The effects of native oxide surface layer on the electrochemical performance of Si nanoparticle-based electrodes, 158(12) (2011) A1260.
[155] X. Zhou, Y.X. Yin, L.J. Wan, Y.G.J.A.E.M. Guo, Self-assembled nanocomposite of silicon nanoparticles encapsulated in graphene through electrostatic attraction for lithium-ion batteries, 2(9) (2012) 1086-1090.
[156] Z. Feng, C. Huang, A. Fu, L. Chen, F. Pei, Y. He, X. Fang, B. Qu, X. Chen, A.M.J.T.S.F. Ng, A three-dimensional network of graphene/silicon/graphene sandwich sheets as anode for Li-ion battery, 693 (2020) 137702.
[157] T. Mori, C.-J. Chen, T.-F. Hung, S.G. Mohamed, Y.-Q. Lin, H.-Z. Lin, J.C. Sung, S.-F. Hu, R.-S.J.E.A. Liu, High specific capacity retention of graphene/silicon nanosized sandwich structure fabricated by continuous electron beam evaporation as anode for lithium-ion batteries, 165 (2015) 166-172.
[158] L. Wei, Z. Hou, H.J.E.A. Wei, Porous sandwiched graphene/silicon anodes for lithium storage, 229 (2017) 445-451.
[159] Z.-F. Li, H. Zhang, Q. Liu, Y. Liu, L. Stanciu, J.J.A.a.m. Xie, interfaces, Novel pyrolyzed polyaniline-grafted silicon nanoparticles encapsulated in graphene sheets as Li-ion battery anodes, 6(8) (2014) 5996-6002.
[160] R. Yi, J. Zai, F. Dai, M.L. Gordin, D.J.N.e. Wang, Dual conductive network-enabled graphene/Si–C composite anode with high areal capacity for lithium-ion batteries, 6 (2014) 211-218.
[161] D.A. Agyeman, K. Song, G.H. Lee, M. Park, Y.M.J.A.e.m. Kang, Carbon-coated Si nanoparticles anchored between reduced graphene oxides as an extremely reversible anode material for high energy-density Li-ion battery, 6(20) (2016) 1600904.
[162] I.H. Son, J. Hwan Park, S. Kwon, S. Park, M.H. Rümmeli, A. Bachmatiuk, H.J. Song, J. Ku, J.W. Choi, J.-m.J.N.c. Choi, Silicon carbide-free graphene growth on silicon for lithium-ion battery with high volumetric energy density, 6(1) (2015) 1-8.
[163] Y. Hwa, W.-S. Kim, S.-H. Hong, H.-J.J.E.A. Sohn, High capacity and rate capability of core–shell structured nano-Si/C anode for Li-ion batteries, 71 (2012) 201-205.
[164] D. Wang, M. Gao, H. Pan, J. Wang, Y.J.J.o.P.S. Liu, High performance amorphous-Si@ SiOx/C composite anode materials for Li-ion batteries derived from ball-milling and in situ carbonization, 256 (2014) 190-199.
[165] X. Chen, X. Yang, F. Pan, T. Zhang, X. Zhu, J. Qiu, M. Li, Y. Mu, H.J.J.o.A. Ming, Compounds, Fluorine-functionalized core-shell Si@ C anode for a high-energy lithium-ion full battery, 884 (2021) 160945.
[166] K. Wang, S. Pei, Z. He, L.-a. Huang, S. Zhu, J. Guo, H. Shao, J.J.C.E.J. Wang, Synthesis of a novel porous silicon microsphere@ carbon core-shell composite via in situ MOF coating for lithium ion battery anodes, 356 (2019) 272-281.
[167] J. Shi, H. Gao, G. Hu, Q.J.J.o.P.S. Zhang, Core-shell structured Si@ C nanocomposite for high-performance Li-ion batteries with a highly viscous gel as precursor, 438 (2019) 227001.
[168] R. Zhou, H. Guo, Y. Yang, Z. Wang, X. Li, Y.J.J.o.A. Zhou, Compounds, N-doped carbon layer derived from polydopamine to improve the electrochemical performance of spray-dried Si/graphite composite anode material for lithium ion batteries, 689 (2016) 130-137.
[169] J. Yang, Y.-X. Wang, S.-L. Chou, R. Zhang, Y. Xu, J. Fan, W.-x. Zhang, H.K. Liu, D. Zhao, S.X.J.N.E. Dou, Yolk-shell silicon-mesoporous carbon anode with compact solid electrolyte interphase film for superior lithium-ion batteries, 18 (2015) 133-142.
[170] X.-y. Zhou, J.-j. Tang, J. Yang, J. Xie, L.-l.J.E.A. Ma, Silicon@ carbon hollow core–shell heterostructures novel anode materials for lithium ion batteries, 87 (2013) 663-668.
[171] L. Yang, H. Li, J. Liu, Z. Sun, S. Tang, M.J.S.r. Lei, Dual yolk-shell structure of carbon and silica-coated silicon for high-performance lithium-ion batteries, 5(1) (2015) 1-9.
[172] M.-S. Wang, L.-Z. Fan, M. Huang, J. Li, X.J.J.o.P.S. Qu, Conversion of diatomite to porous Si/C composites as promising anode materials for lithium-ion batteries, 219 (2012) 29-35.
[173] W. Ren, Z. Zhang, Y. Wang, Q. Tan, Z. Zhong, F.J.J.o.M.C.A. Su, Preparation of porous silicon/carbon microspheres as high performance anode materials for lithium ion batteries, 3(11) (2015) 5859-5865.
[174] J.-l. Liu, X.-m. Wu, S. Chen, R.-l. Long, C.-s. Yin, F.J.S. Zhang, Phenolic Resin-coated Porous Silicon/carbon Microspheres Anode Materials for Lithium-ion Batteries, (2021) 1-8.
[175] P.-L. Taberna, S. Mitra, P. Poizot, P. Simon, J.-M.J.N.m. Tarascon, High rate capabilities Fe_3O_4-based Cu nano-architectured electrodes for lithium-ion battery applications, 5(7) (2006) 567-573.
[176] J.-M. Tarascon, S. Grugeon, M. Morcrette, S. Laruelle, P. Rozier, P.J.C.R.C. Poizot, New concepts for the search of better electrode materials for rechargeable lithium batteries, 8(1) (2005) 9-15.
[177] P. Poizot, S. Laruelle, S. Grugeon, J.-M.J.J.o.T.E.S. Tarascon, Rationalization of the low-potential reactivity of 3d-metal-based inorganic compounds toward Li, 149(9) (2002) A1212.
[178] P. Poizot, S. Laruelle, S. Grugeon, L. Dupont, J.J.N. Tarascon, Nano-sized transition-metal oxides as negative-electrode materials for lithium-ion batteries, 407(6803) (2000) 496-499.
[179] S. Fang, D. Bresser, S.J.T.M.O.f.E.E.S. Passerini, Transition metal oxide anodes for electrochemical energy storage in lithium-and sodium-ion batteries, (2022) 55-99.
[180] M. Hong, Y. Su, C. Zhou, L. Yao, J. Hu, Z. Yang, L. Zhang, Z. Zhou, N. Hu, Y.J.J.o.A. Zhang, Compounds, Scalable synthesis of γ-Fe_2O_3/CNT composite as high-performance anode material for lithium-ion batteries, 770 (2019) 116-124.
[181] P. Peng, Q. Zhao, P. Zhu, W. Liu, Y. Yuan, R. Ding, P. Gao, X. Sun, E.J.J.o.E.C. Liu, Amorphous Fe_2O_3 film-coated mesoporous Fe_2O_3 core-shell nanosphere prepared by quenching as a high-performance anode material for lithium-ion batteries, 898 (2021) 115633.
[182] Y. Huang, Z. Lin, M. Zheng, T. Wang, J. Yang, F. Yuan, X. Lu, L. Liu, D.J.J.o.P.S. Sun, Amorphous Fe_2O_3 nanoshells coated on carbonized bacterial cellulose nanofibers as a flexible anode for high-performance lithium ion batteries,

307 (2016) 649-656.
[183] X. Qi, Z. Yan, Y. Liu, X. Li, G. He, S.J.M.C. Komarneni, Physics, Ni and Co doped yolk-shell type Fe_2O_3 hollow microspheres as anode materials for lithium-ion batteries, 211 (2018) 452-461.
[184] H. Kong, C. Lv, C. Yan, G.J.I.C. Chen, Engineering mesoporous single crystals Co-doped Fe_2O_3 for high-performance lithium ion batteries, 56(14) (2017) 7642-7649.
[185] M. Reddy, T. Yu, C.-H. Sow, Z.X. Shen, C.T. Lim, G. Subba Rao, B.J.A.F.M. Chowdari, α-Fe_2O_3 nanoflakes as an anode material for Li-ion batteries, 17(15) (2007) 2792-2799.
[186] Z. Zheng, P. Li, J. Huang, H. Liu, Y. Zao, Z. Hu, L. Zhang, H. Chen, M.-S. Wang, D.-L.J.J.o.E.C. Peng, High performance columnar-like Fe_2O_3@ carbon composite anode via yolk@ shell structural design, 41 (2020) 126-134.
[187] Y. Li, T.-F. Yi, X. Li, X. Lai, J. Pan, P. Cui, Y.-R. Zhu, Y.J.C.I. Xie, Li2ZnTi3O8@ α-Fe_2O_3 composite anode material for Li-ion batteries, 47(13) (2021) 18732-18742.
[188] J. Wang, X. Yang, Y. Wang, S. Jin, W. Cai, B. Liu, C. Ma, X. Liu, W. Qiao, L.J.C.E.S. Ling, Rational design and synthesis of sandwich-like reduced graphene oxide/Fe_2O_3/N-doped carbon nanosheets as high-performance anode materials for lithium-ion batteries, 231 (2021) 116271.
[189] S. Ullah, B.D. Campéon, S. Ibraheem, G. Yasin, R. Pathak, Y. Nishina, T.A. Nguyen, Y. Slimani, Q.J.J.o.I. Yuan, E. Chemistry, Enabling the fast lithium storage of large-scalable γ-Fe_2O_3/Carbon nanoarchitecture anode material with an ultralong cycle life, 101 (2021) 379-386.
[190] Z. Zheng, Y. Zao, Q. Zhang, Y. Cheng, H. Chen, K. Zhang, M.-S. Wang, D.-L.J.C.E.J. Peng, Robust erythrocyte-like Fe_2O_3@ carbon with yolk-shell structures as high-performance anode for lithium ion batteries, 347 (2018) 563-573.
[191] X. Yan, F. Jiang, X. Sun, R. Du, M. Zhang, L. Kang, Q. Han, W. Du, D. You, Y.J.J.o.A. Zhou, Compounds, A simple, low-cost and scale-up synthesis strategy of spherical-graphite/Fe_2O_3 composites as high-performance anode materials for half/full lithium ion batteries, 822 (2020) 153719.
[192] J.S. Cho, Y.J. Hong, Y.C.J.A.n. Kang, Design and synthesis of bubble-nanorod-structured Fe_2O_3–carbon nanofibers as advanced anode material for Li-ion batteries, 9(4) (2015) 4026-4035.
[193] Y. Cheng, G. Chen, H. Wu, M. Zhu, Y.J.J.o.M.C.A. Lu, Use of regenerated cellulose to direct hetero-assembly of nanoparticles with carbon nanotubes for producing flexible battery anodes, 5(27) (2017) 13944-13949.
[194] P. Bhattacharya, M. Kota, D.H. Suh, K.C. Roh, H.S.J.A.E.M. Park, Biomimetic Spider-Web-Like Composites for Enhanced Rate Capability and Cycle Life of Lithium Ion Battery Anodes, 7(17) (2017) 1700331.
[195] G. Zhou, D.-W. Wang, P.-X. Hou, W. Li, N. Li, C. Liu, F. Li, H.-M.J.J.o.M.C. Cheng, A nanosized Fe_2O_3 decorated single-walled carbon nanotube membrane as a high-performance flexible anode for lithium ion batteries, 22(34) (2012) 17942-17946.
[196] Q. Guo, P. Guo, J. Li, H. Yin, J. Liu, F. Xiao, D. Shen, N.J.J.o.S.S.C. Li, Fe_3O_4–CNTs nanocomposites: inorganic dispersant assisted hydrothermal synthesis and application in lithium ion batteries, 213 (2014) 104-109.
[197] Y. He, L. Huang, J.-S. Cai, X.-M. Zheng, S.-G.J.E.A. Sun, Structure and electrochemical performance of nanostructured Fe_3O_4/carbon nanotube composites as anodes for lithium ion batteries, 55(3) (2010) 1140-1144
[198] X. Li, D. Li, Z. Wei, X. Shang, D.J.E.A. He, Interconnected MnO_2 nanoflakes supported by 3D nanostructured stainless steel plates for lithium ion battery anodes, 121 (2014) 415-420.
[199] M. Liu, L. Gan, W. Xiong, Z. Xu, D. Zhu, L.J.J.o.M.C.A. Chen, Development of MnO 2/porous carbon microspheres with a partially graphitic structure for high performance supercapacitor electrodes, 2(8) (2014) 2555-2562.
[200] J. Zhang, A.J.S.B. Yu, Nanostructured transition metal oxides as advanced anodes for lithium-ion batteries, 60(9) (2015) 823-838.
[201] W. Mao, G. Ai, Y. Dai, Y. Fu, Y. Ma, S. Shi, R. Soe, X. Zhang, D. Qu, Z.J.J.o.P.S. Tang, In-situ synthesis of MnO_2@ CNT microsphere composites with enhanced electrochemical performances for lithium-ion batteries, 310 (2016) 54-60.
[202] Y. Fan, G. Clavel, N.J.J.o.N.R. Pinna, Effect of passivating Al_2O_3 thin films on MnO_2/carbon nanotube composite lithium-ion battery anodes, 20(8) (2018) 1-11.
[203] G. Wang, X. Shen, J.J.J.o.P.S. Yao, One-dimensional nanostructures as electrode materials for lithium-ion batteries with improved electrochemical performance, 189(1) (2009) 543-546.
[204] M. Xu, F. Wang, Y. Zhang, S. Yang, M. Zhao, X.J.N. Song, Co3O4–carbon nanotube heterostructures with bead-on-string architecture for enhanced lithium storage performance, 5(17) (2013) 8067-8072.
[205] N.T.M. Hao, S. Ahmed, J.C. An, H.J. Sun, G. Park, J.J.B.o.t.K.C.S. Shim, Co-Co3O4 Embedded in Carbon Nanotube Derived from a Zeolitic-Imidazolate Framework as Anode Material for Lithium-Ion Batteries, 42(9) (2021) 1220-1224.
[206] Y. Fu, R. Ma, Y. Shu, Z. Cao, X.J.M.L. Ma, Preparation and characterization of SnO_2/carbon nanotube composite for lithium ion battery applications, 63(22) (2009) 1946-1948.
[207] Z. Wen, Q. Wang, Q. Zhang, J.J.A.F.M. Li, In situ growth of mesoporous SnO_2 on multiwalled carbon nanotubes: A novel composite with porous-tube structure as anode for lithium batteries, 17(15) (2007) 2772-2778.
[208] G. Chen, Z. Wang, D.J.C.o.M. Xia, One-pot synthesis of carbon nanotube@ SnO_2− Au coaxial nanocable for lithium-ion batteries with high rate capability, 20(22) (2008) 6951-6956.
[209] I. Elizabeth, A.K. Nair, B.P. Singh, S.J.E.A. Gopukumar, Multifunctional Ni-NiO-CNT composite as high performing free standing anode for Li ion batteries and advanced electro catalyst for oxygen evolution reaction, 230 (2017) 98-105.
[210] Y. Xu, S. Hou, G. Yang, T. Lu, L.J.J.o.S.S.E. Pan, NiO/CNTs derived from metal-organic frameworks as superior anode material for lithium-ion batteries, 22(3) (2018) 785-795.
[211] Y. Yin, Y. Jia, X. Zhang, C. Ma, Z. Sun, S.J.J.o.A.E. Yang, Facile synthesis of NiO/MWCNT composites by a vacuum solution infiltration method for lithium-ion batteries, 44(11) (2014) 1185-1191.
[212] L.-H. Wang, X.-L. Teng, Y.-F. Qin, Q.J.C.I. Li, High electrochemical performance and structural stability of CoO nanosheets/CoO film as self-supported anodes for lithium-ion batteries, 47(4) (2021) 5739-5746.
[213] Q. Li, Y. Zhao, H. Liu, P. Xu, L. Yang, K. Pei, Q. Zeng, Y. Feng, P. Wang, R.J.A.n. Che, Dandelion-like Mn/Ni Co-doped CoO/C hollow microspheres with oxygen vacancies for advanced lithium storage, 13(10) (2019) 11921-11934.
[214] L. Xu, C. Wang, D. Deng, Y. Tian, X. He, G. Lu, J. Qian, S. Yuan, H.J.A.S.C. Li, Engineering, Cobalt oxide nanoparticles/nitrogen-doped graphene as the highly efficient oxygen reduction electrocatalyst for rechargeable zinc-air batteries, 8(1) (2019) 343-350.
[215] Y. Pang, S. Chen, C. Xiao, S. Ma, S.J.J.o.M.C.A. Ding, MOF derived CoO-NCNTs two-dimensional networks for durable lithium and sodium storage, 7(8) (2019) 4126-4133.
[216] C. Zhou, J. Liu, S. Guo, P. Zhang, S. Li, Y. Yang, J. Wu, L. Chen, M.J.C. Wang, Nanoporous CoO Nanowire Clusters Grown on Three-Dimensional Porous Graphene Cloth as Free-Standing Anode for Lithium-Ion Batteries, 7(7) (2020) 1573-1580.
[217] Y. Hu, Z. Li, Z. Hu, L. Wang, R. Ma, J.J.S. Wang, Engineering hierarchical CoO nanospheres wrapped by graphene via controllable sulfur doping for superior Li ion storage, 16(42) (2020) 2003643.
[218] L. Tan, X. Lan, R. Hu, J. Liu, B. Yuan, M.J.C. Zhu, Stable Lithium Storage at Subzero Temperatures for High-capacity Co3O4@ graphene Composite Anodes, 7(1) (2021) 61-70.
[219] J. Fu, W. Kang, X. Guo, H. Wen, T. Zeng, R. Yuan, C.J.J.o.E.C. Zhang, 3D hierarchically porous NiO/Graphene hybrid paper anode for long-life and high rate cycling flexible Li-ion batteries, 47 (2020) 172-179.
[220] D.R. Deng, Q.H.J.C. Wu, In-Situ Synthesis Graphene Supported TiO_2 Nanosheets with Superior Cyclic and Rate Performance for Lithium-Ion Batteries, 5(40) (2020) 12425-12429.
[221] F. Gong, Q. Zhou, J. Liu, D. Wang, S. Wu, D.D.J.E. Xia, Fuels, Facile and controllable synthesis of $Co_2V_2O_7$ microplatelets anchored on graphene layers toward superior Li-Ion battery anodes, 34(6) (2020) 7616-7621.
[222] H. Shen, X. Xia, S. Yan, X. Jiao, D. Sun, W. Lei, Q.J.J.o.A. Hao, Compounds, SnO_2/$NiFe_2O_4$/graphene nanocomposites as anode materials for lithium ion batteries, 853 (2021) 157017.
[223] Y. Lin, J. Wu, X. Huang, G. Pan, X.J.J.o.E.C. Xia, Boosting fast lithium ion storage of Li4Ti5O12 by synergistic effect of vertical graphene and nitrogen doping, 51 (2020) 372-377.
[224] R. Menéndez, P. Alvarez, C. Botas, F. Nacimiento, R. Alcántara, J.L. Tirado, G.F.J.J.o.P.S. Ortiz, Self-organized amorphous titania nanotubes with deposited graphene film like a new heterostructured electrode for lithium ion batteries, 248 (2014) 886-893.
[225] J. Shao, H. Zhou, J. Feng, M. Zhu, A.J.J.o.A. Yuan, Compounds, Facile synthesis of MOF-derived hollow NiO microspheres integrated with graphene foam for improved lithium-storage properties, 784 (2019) 869-876.
[226] C. Zhang, H.B. Wu, Z. Guo, X.W.D.J.E.C. Lou, Facile synthesis of carbon-coated MoS2 nanorods with enhanced lithium storage properties, 20 (2012) 7-10.
[227] H. Li, L. Ma, W.-x. Chen, J.-m.J.M.L. Wang, Synthesis of MoS2/C nanocomposites by hydrothermal route used as Li-ion intercalation electrode materials, 63(15) (2009) 1363-1365.
[228] L. Fei, Y. Xu, X. Wu, G. Chen, Y. Li, B. Li, S. Deng, S. Smirnov, H. Fan,

H.J.N. Luo, Instant gelation synthesis of 3D porous MoS 2@ C nanocomposites for lithium ion batteries, 6(7) (2014) 3664-3669.
[229] S. Ding, J.S. Chen, X.W.J.C.A.E.J. Lou, Glucose-assisted growth of MoS2 nanosheets on CNT backbone for improved lithium storage properties, 17(47) (2011) 13142-13145
[230] S.-K. Park, S.-H. Yu, S. Woo, B. Quan, D.-C. Lee, M.K. Kim, Y.-E. Sung, Y.J.D.T. Piao, A simple l-cysteine-assisted method for the growth of MoS 2 nanosheets on carbon nanotubes for high-performance lithium ion batteries, 42(7) (2013) 2399-2405.
[231] X. Zhou, L.-J. Wan, Y.-G.J.C.c. Guo, Synthesis of MoS 2 nanosheet–graphene nanosheet hybrid materials for stable lithium storage, 49(18) (2013) 1838-1840.
[232] K. Chang, D. Geng, X. Li, J. Yang, Y. Tang, M. Cai, R. Li, X.J.A.E.M. Sun, Ultrathin MoS2/nitrogen-doped graphene nanosheets with highly reversible lithium storage, 3(7) (2013) 839-844.
[233] H.S. Kim, Y.H. Chung, S.H. Kang, Y.-E.J.E.A. Sung, Electrochemical behavior of carbon-coated SnS2 for use as the anode in lithium-ion batteries, 54(13) (2009) 3606-3610.
[234] H. Sun, M. Ahmad, J. Luo, Y. Shi, W. Shen, J.J.M.R.B. Zhu, SnS2 nanoflakes decorated multiwalled carbon nanotubes as high performance anode materials for lithium-ion batteries, 49 (2014) 319-324.
[235] J.-G. Kang, G.-H. Lee, K.-S. Park, S.-O. Kim, S. Lee, D.-W. Kim, J.-G.J.J.o.M.C. Park, Three-dimensional hierarchical self-supported multi-walled carbon nanotubes/tin (iv) disulfide nanosheets heterostructure electrodes for high power Li ion batteries, 22(18) (2012) 9330-9337.
[236] B. Luo, Y. Fang, B. Wang, J. Zhou, H. Song, L.J.E. Zhi, E. Science, Two dimensional graphene–SnS 2 hybrids with superior rate capability for lithium ion storage, 5(1) (2012) 5226-5230.
[237] K. Chang, Z. Wang, G. Huang, H. Li, W. Chen, J.Y.J.J.o.P.S. Lee, Few-layer SnS2/graphene hybrid with exceptional electrochemical performance as lithium-ion battery anode, 201 (2012) 259-266.
[238] C.S. Rout, B.-H. Kim, X. Xu, J. Yang, H.Y. Jeong, D. Odkhuu, N. Park, J. Cho, H.S.J.J.o.t.A.C.S. Shin, Synthesis and characterization of patronite form of vanadium sulfide on graphitic layer, 135(23) (2013) 8720-8725.
[239] B. Long, M.S. Balogun, L. Luo, Y. Luo, W. Qiu, S. Song, L. Zhang, Y.J.S. Tong, Encapsulated vanadium-based hybrids in amorphous N-doped carbon matrix as anode materials for lithium-ion batteries, 13(41) (2017) 1702081.